Co-Optimisation of Electrical and District Heating Networks

Sai Pavan Polisetty

Submitted in partial fulfillment of the requirements for the degree of

Doctor of Philosophy

Imperial College London

Department of Electrical and Electronic Engineering

Control and Power Research Group

July 2025

Dedicated to my parents

Bhagya Lakshmi

and

Srinivasa Rao

Declaration of originality

I hereby declare that all the work in this thesis is my own. The work of others has been properly acknowledged.

Sai Pavan Polisetty

July 2025

Declaration of copyright

The copyright of this thesis rests with the author. Unless otherwise indicated, its contents are licensed under a Creative Commons Attribution-Non Commercial-No Derivatives 4.0 International Licence (CC BY-NC-ND).

Under this licence, you may copy and redistribute the material in any medium or format on the condition that; you credit the author, do not use it for commercial purposes and do not distribute modified versions of the work.

When reusing or sharing this work, ensure you make the licence terms clear to others by naming the licence and linking to the licence text.

Please seek permission from the copyright holder for uses of this work that are not included in this licence or permitted under UK Copyright Law.

Abstract

With the growing demand for energy, the interdependence among multiple energy domains is increasing rapidly. This interconnection enables enhanced operational flexibility and cost-effectiveness, but also introduces significant complexity due to the intermittent and stochastic nature of renewable energy sources (RES). Integrated energy systems are drawing huge attention for their potential to enable efficient and sustainable energy management across sectors. However, the optimal dispatch of the different energy sources, storage systems, and flexible loads in such systems remains a significant challenge.

This thesis presents a two-part investigation into the co-optimisation of distribution-level integrated energy systems comprising coupled electrical distribution networks and district heating networks. In the first part, a linear co-optimisation framework is developed to schedule the dispatch of energy resources based on day-ahead forecasts of RES generation and energy demands. Electric boilers and heaters are employed as coupling devices between the two networks. By leveraging the inherent flexibility in both domains, the proposed model minimises operational costs and renewable curtailment. A case study based on the integrated electrical and heating system at Bornholm Island, Denmark, demonstrates the effectiveness of the approach, showing significant reductions in RES curtailment.

The second part addresses the operational uncertainties associated with RES generation and load forecasts in distribution-level integrated systems. Variability in RES generation, coupled with fluctuations in electrical and thermal demands, can lead to significant operational challenges, including voltage deviations, temperature constraint violations, and inefficient resource utilisation. A rule-based dynamic dispatch is proposed to handle the increasing levels of uncertain RES. A chance-constrained (CC) co-optimisation algorithm considering the uncertain loads and RES is developed. The analysis is conducted using snapshot-based simulations of representative operating conditions. In the proposed method, electric boiler power and curtailment of RES are dynamically dispatched to reduce operational costs and network losses. The

approach is validated on the IEEE 15-bus distribution system and the UK Generic Distribution System (UKGDS) 95-bus test systems. The results show that the developed method significantly reduces the voltage deviations and temperature violations compared to the deterministic method.

Together, these contributions provide a comprehensive framework for the economical operation of integrated electrical and thermal energy systems in the presence of increasing renewable energy penetration.

Acknowledgement

This work has been carried out under the supervision of Prof. Bikash Pal of Imperial College. I express my sincere gratitude to him for his continuous guidance, support, ideas, and time throughout the doctoral program. I highly appreciate his generosity and encouragement, which have been instrumental to my development as a researcher. Besides being an excellent mentor, he is a great human being.

I would also like to deeply thank Dr. Firdous Ul Nazir and Dr. Thomas Joseph, who have continuously helped with their expert advice throughout my PhD journey. Without their technical inputs and support, completing this research within the desired time frame would have been very difficult. Their prompt and insightful responses were pivotal to the successful completion of this work.

My sincere thanks to the wonderful group of colleagues at the Control and Power research group who created a supportive environment throughout my studies. Special mention to Sowmya, Carlos, Eduardo, Mert, Andreas, Malek, Ali, Fatemeh, Ambuj, Fahim, and Lorenzo. It was a pleasure to work and learn alongside such a dynamic and collaborative team. I appreciate the camaraderie of my close friends from Imperial and beyond, Anudeep, Hithesh, Swathi, Shyamala, Veen, Gautham, and Anju, whose company made this journey enjoyable and well-balanced.

I would like to take this opportunity to thank my family for their unwavering love and support. To my mom and dad, who supported me in all pursuits with unconditional love and encouragement. To my younger brother, Tarun, whose presence adds laughter and energy to our family life, and whose enthusiasm for life keeps me grounded. Finally, I gratefully acknowledge the European Union's Horizon 2020 Research and Innovation Program and the Department of Science and Technology (DST), India, for sponsoring this PhD through the RE-EMPOWERED Project under Grant Agreement No. 101018420 and DST/TMD/INDIA/EU/ILES/2020/50(c), respectively.

Contents

Declaration of originality **3**

Declaration of copyright **4**

Abstract **4**

Acknowledgement **6**

List of figures **11**

List of tables **13**

Nomenclature **13**

1 Introduction **17**

1.1 Motivation 18

1.2 Literature review of electrical and heating systems 21

1.2.1 Optimal power flow in IEHS 22

1.2.2 Scheduling under uncertainty 24

1.3 Limitations of existing works 26

1.4 Objectives and contributions 27

1.4.1 Original contributions 29

1.4.2 Research dissemination 30
1.5 Organisation of the thesis 31

2 Scheduling of integrated electrical and heating systems 34

2.1 Electric power system 35
2.2 District heating system 36
2.3 Coupling strategy and independent optimisation cases 38
2.4 Linear co-optimisation of IEHS systems 39
2.4.1 Cost function 39
2.5 Simulation results 41
2.6 Conclusions 47

3 Chance-constrained co-optimisation of IEHS 50

3.1 Introduction 50
3.2 Electrical and heating system modelling 51
3.2.1 Electrical power flow modelling 52
3.2.2 Thermal power flow modelling 54
3.3 Deterministic formulation 57
3.4 Chance-constrained co-optimisation formulation 59
3.5 Dynamic dispatch of curtailments and electric boiler power 61
3.6 Scenario reduction methodology 62
3.7 Solution methodology for the co-optimisation of IEHS 65
3.7.1 Steps involved in the algorithm 66

3.7.2 Conclusions 68

4 Numerical results **69**

4.1 Introduction 69

4.2 System model 70

4.3 Solution using deterministic approach 71

4.3.1 Discussion on relaxation gap 74

4.3.2 Solution using chance-constrained approach 75

4.4 Conclusions 81

5 Conclusions and future work **85**

5.1 Conclusions 86

5.2 Future work 87

Appendices **99**

A 5-bus DHS system data **100**

A.1 Heat network pipe parameters 100

A.2 Source and load details 101

B IEEE 15-bus system data **102**

C 95-bus UKGDS data **105**

List of Figures

1.1 Historical and future cumulative solar PV and wind power capacity 18
1.2 UK wind deployment and curtailment costs on the Scotland-England boundary . 19
1.3 Multi energy system with various sources, storages, and loads 21

2.1 DHS at Bornholm consisting of heating plant and consumers 36
2.2 Interconnection between EPS and DHS at Bornholm 39
2.3 Typical generation and load profiles for a day at Bornholm 42
2.4 Total electrical and heat power generation and demand in the island for case 1 . 44
2.5 Total electrical and heat power generation and demand in the island for case 2 . 45
2.6 Total electrical and heat power generation and demand in the island for case 3 . 47

3.1 Line model in a distribution system 52
3.2 Pipes representation in district heating system 55
3.3 Flowchart for the chance-constrained optimisation 67

4.1 IEEE 15 bus test system 71
4.2 A 5-bus district heating test system 71
4.3 UKGDS 95-bus test system 72
4.4 Voltage and temperature violations for the 15-bus system with deterministic dispatch 73
4.5 Relaxation gap of the inequality constraint of each branch for IEEE 15-bus deterministic case 73
4.6 Voltage and temperature violations for the 95-bus system with deterministic dispatch 74

4.7 Relaxation gap of the inequality constraint of each branch for UKGDS 95-bus deterministic case 75
4.8 Comparison of expected values of 15-bus (a) electric boiler power (b)curtailments 76
4.9 Voltage and temperature violations at each iteration for the 15-bus system with SD=0.2 77
4.10 Comparison of violations in the posterior set for 15-bus DET and CC cases (a) voltage violations (b) temperature violations 78
4.11 Comparison of expected values of 95-bus (a) electric boiler power (b) curtailments 79

List of Tables

2.1 Simulation parameters 43

2.2 Comparison of independent optimisation and co-optimisation for case 1 48

2.3 Comparison of independent optimisation and co-optimisation for case 2 49

4.1 Percentage of scenarios passed using deterministic approach for 15-bus test system 74

4.2 Summary of scenarios passed and violations for 15-bus test system 77

4.3 Number of iterations and reduced scenarios for 15-bus system 79

4.4 Coefficients of the dynamic dispatch variables of the 15-bus test system for different SDs 80

4.5 Dynamic dispatch coefficients of the 15-bus test system for different locations of DHS network 81

4.6 Summary of scenarios passed and violations for 95-bus test system 82

4.7 Coefficients of the dynamic dispatch variables of the 95-bus test system for different SD's 83

4.8 Number of iterations and reduced scenarios for 95-bus system 83

4.9 Dynamic dispatch coefficients of the 95-bus test system for different locations of DHS network 84

B.1 15-bus system line data: resistance and reactance (pu) 102

B.2 15-bus system line data: active and reactive power flow (pu) 103

C.1 95-bus UKGDS line data 105

C.2 95-bus UKGDS load data 111

Nomenclature

η Efficiency of the electrical boiler

A_T Incidence matrix of the thermal network

APC Active power control

B_E Set of all the electrical network branches

B_R Set of all the electrical buses where RES is installed

B_T Set of all the thermal network branches

B_{EB} Set of all the electrical buses where EB is installed

CC Chance constrained

$CFVT$ Constant flow variable temperature

CI Current injection

DHS District heating system

EB Electric boiler

EPS Electrical power system

$IEHS$ Integrated electrical and thermal system

N_E Set of all the electrical load nodes

N_T Set of all the thermal load nodes

OPF Optimal power flow

$P(x)$ Probability of occurrence of an event

R_{CC} Set of random scenarios considered for chance-constrained optimisation

RES Renewable energy sources

RPC Reactive power control

SSR Submodular scenario reduction

x_{min}/x_{max} Minimum/maximum value of quantity x

π_i Probability of occurrence of a scenario i

N_{min} Minimum number of scenarios considered in the objective function

p_{gj} Real power generated at node j

p_{gj}^f Real power forecast of the generation at node j

p_{lj} Real power demand at node j

p_{lj}^f Real power forecast of the load at node j

r_{ij} resistance of the line ij

s_{gj} Complex power injected by DG at bus j

s_j Complex power demand at node j

$T_i^{'}$ Temperature at node i of the return pipe

x_{ij} reactance of the line ij

z_{ij} Impedance of the line ij

$\dot{m}_i$ Net mass flow rate consumption at node i

$\dot{m}_i^p$ Mass flow rate in supply pipe i

ϵ Acceptable probability of constraint violation in the chance-constrained optimisation framework.

γ Probability that the scenario-based guarantee fails

A, B Dynamic dispatch rule matrices

I_{ij} Branch current flow in line ij

l_{ij} Squared current magnitude flowing in line ij

p_{cj}^d Dispatch of curtailed power at node j

P_{ij} Real power flowing in line ij

Q_{ij} Reactive power flowing in line ij

S_{ij} Complex power flow in line ij

T_i Temperature at node i of the supply pipe

T_i^{p+} Outflow temperature of supply pipe i

T_i^{p-} Inflow temperature of supply pipe i

V_i Voltage at node i

v_i Squared voltage magnitude at node i

Chapter 1

Introduction

The global energy landscape is undergoing a rapid transformation, driven by escalating climate concerns and reinforced by international net-zero targets such as those set by the Paris Agreement and reinforced at COP28. Global capacities of solar and wind installations (in GW) from 2018 to 2030 (planned) are as shown in Fig. 1.1. Renewable energy sources (RES), particularly wind and solar, are at the core of this transition, offering low-carbon electricity generation. However, their inherent intermittent and uncertain nature poses significant operational challenges. In many regions, the mismatch between rapid renewable deployment and slow infrastructure upgrades has led to increased curtailment of clean energy, around 4% in the UK in 2022 alone, with projections reaching up to 20% by 2030 [1]. Without timely and strategic integration measures, studies suggest that up to 15% of global wind and solar generation could be lost by 2030, leading to substantial setbacks in emissions reduction efforts [2]. This situation underscores the urgent need for more flexible, integrated approaches to energy system planning and operation.

In the context of the UK, the wind capacity expansion and curtailment costs are increasing year on year as shown in Fig. 1.2 [3]. This growing curtailment not only leads to significant economic losses and wasted clean energy but also risks undermining investor confidence in

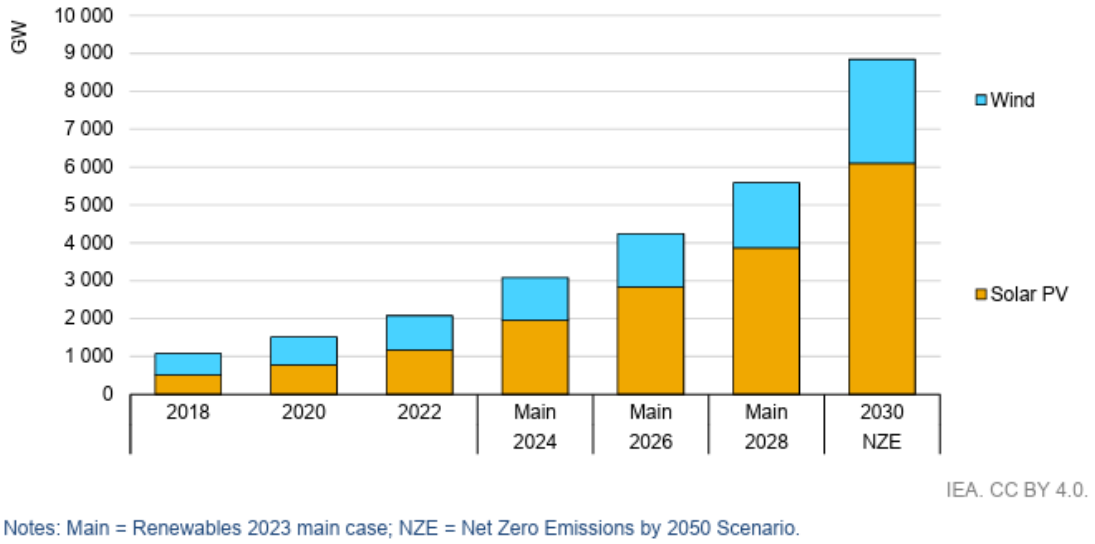


Figure 1.1: Historical and future cumulative solar PV and wind power capacity [2]

renewable projects. One promising solution to this challenge is the deployment of multi-energy systems (MES), which directly address renewable curtailment by enabling surplus electrical energy to be converted, shifted, and stored in other energy vectors. By integrating electricity, heating, and gas networks, MES can unlock new flexibility pathways that reduce curtailment and improve energy utilisation.

1.1 Motivation

Integrated energy systems (IES), or more broadly, multienergy systems (MES), offer a promising paradigm shift by enabling coordinated management of multiple energy vectors like electricity, heat, and gas across generation, storage, and consumption. These systems exploit interdependencies between vectors to enhance system flexibility, reduce RES curtailment, and unlock new pathways for demand-side and intertemporal arbitrage. A prominent example is the integration of electrical and district heating systems (DHS). DHS are centralised energy networks that produce and distribute thermal energy, which is typically in the form of hot water or steam, to meet the heating demands of residential, commercial, and public buildings. In integrated electrical and heating systems (IEHS), the excess electricity from renewables can be converted

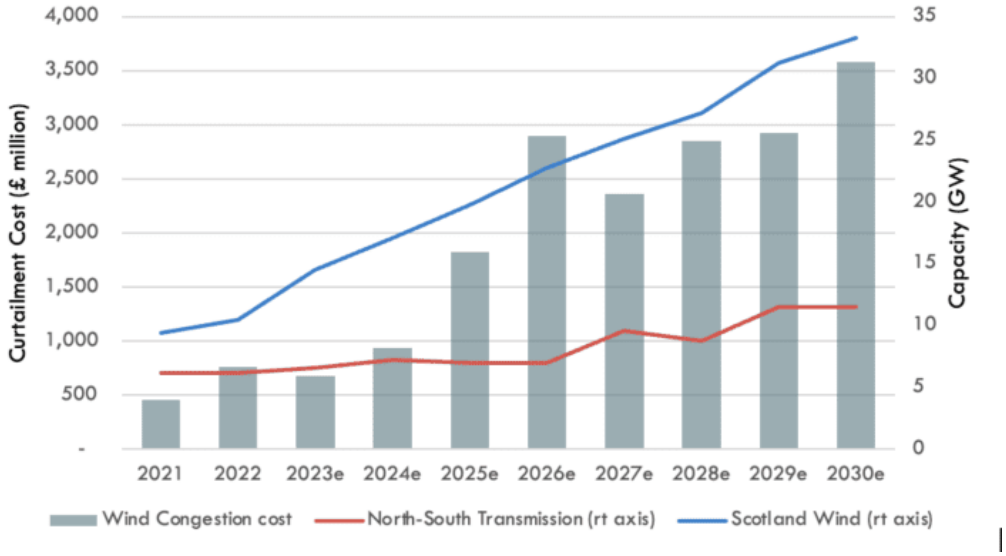


Figure 1.2: UK wind deployment and curtailment costs on the Scotland-England boundary [3]

into heat via electric boilers or heat pumps, stored thermally, and later used to meet heating demands. Such coupling not only increases system-wide efficiency but also offers novel avenues for decarbonising the heating sector, which accounts for nearly 50% of global energy consumption [4]. Despite its importance, renewable heat consumption is expected to grow by just over 40% between 2023 and 2028, which is about two-thirds of the increase in total heat demand. As a result, fossil fuel use for heating is projected to rise further, leading to a 5% increase in annual CO_2 emissions and adding approximately 86 Gt CO_2 cumulatively during this period. Accelerating the integration of renewable electricity into heating systems through MES is thus essential to meeting global climate targets and reducing heat-related emissions.

In recent years, there has been a growing interest in the coordinated operation of multiple energy systems with interconnecting elements [5]. Developments in smart grids and urban energy infrastructures have further highlighted the relevance of MES in supporting the evolving needs of modern energy systems. Smart cities, in particular, are characterised by a high degree of energy vector diversity, incorporating solar PV, wind, electric vehicles, heat networks, and gas infrastructure on the supply side, as well as flexible loads and storage on the demand side. With the increasing integration of intermittent renewable energy sources, accurate modelling and management of uncertainty in energy scheduling are critical. The limited pace of grid expansion

has exacerbated curtailment issues, especially in high-penetration RES regions. Inaccurate curtailment estimation can lead to system-level operational issues such as voltage violations in the distribution electrical networks and temperature constraint violations in coupled thermal networks. Therefore, active curtailment control mechanisms are essential for safe and reliable system operation.

This thesis focuses on distribution-level electrical networks and district heating systems, where renewable integration challenges, flexibility constraints, and operational uncertainties are most pronounced. Among the various energy vectors, district heating presents a cost-effective and energy-efficient solution for meeting space heating and hot water requirements in residential and commercial buildings. However, as reported by the IEA, approximately 90% of the heat supplied through district heating networks is still generated from fossil fuels, particularly in countries like China and Russia [6]. In the context of smart grids and smart cities, where multiple energy carriers such as electricity, heat, and gas coexist on both the supply and demand sides, co-optimisation of resources becomes critical. By enabling joint scheduling of generation units, storage devices, and flexible loads, MES frameworks can significantly enhance energy utilisation and help mitigate the intermittency of renewable sources. Moreover, co-optimisation supports the efficient use of surplus or otherwise underutilised energy carriers, contributing to optimal demand satisfaction. The system's flexibility stems primarily from three components: storage technologies, interconnecting conversion devices, and responsive demand-side elements.

Optimal scheduling of these diverse energy resources is essential to enhance overall system efficiency, resilience, and sustainability. However, the presence of interdependent networks, stochastic RES, and variable demand patterns significantly complicates this scheduling problem. As a result, MES scheduling becomes a complex, multi-domain challenge that demands advanced optimisation tools capable of dynamically allocating energy resources and flexibility across vectors, while satisfying the operational constraints. A brief literature overview is discussed in the following section.

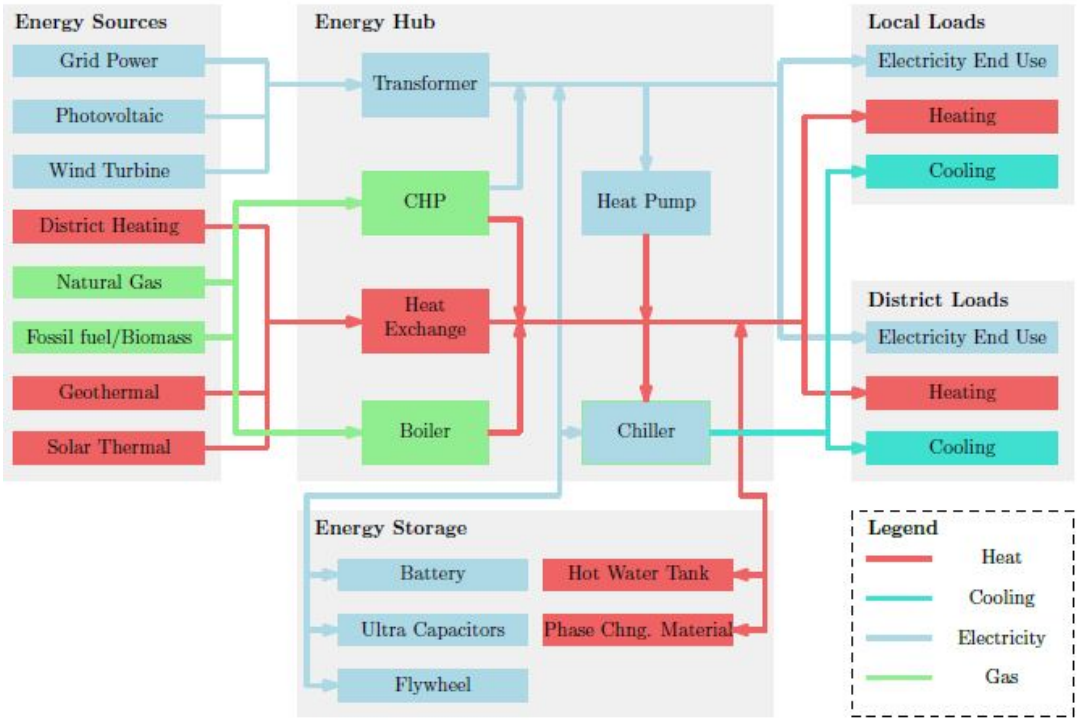


Figure 1.3: Multi energy system with various sources, storages, and loads [7]

1.2 Literature review of electrical and heating systems

This section provides a brief literature overview on the modelling, optimal power flow, and scheduling of MES and IEHS in particular. The modelling of MES has evolved significantly in recent years to capture the growing interdependence between energy vectors such as electricity, heat, gas, and hydrogen. Fig. 1.3 represents an energy hub model of MES with various sources, storages, and loads [7]. Early approaches often considered individual energy carriers in isolation, resulting in suboptimal system-level decisions. More recent works adopt integrated frameworks that model energy conversion, storage, and transport across networks, enabling a holistic representation of MES operations.

One of the foundational contributions in this domain is the energy hub model proposed in [8], which introduces a generalised multi-port node framework to represent energy input/output exchanges across domains. Within this framework, different energy conversions take place inside the hub, and optimal dispatch algorithms determine the conversion levels and energy flows to

meet multi-vector demands. In the existing literature, various algorithms have been discussed to operate MES efficiently. Most of these works differ in the modelling complexity of MES components and in the objectives used for optimisation. Common solution approaches include linear programming, mixed-integer formulations, dynamic programming, genetic algorithms, and Lagrangian relaxation methods [9–14]. A general review of energy management and control strategies is discussed in [15]. A detailed review on modelling and optimal scheduling in IES is attempted in [16].

Recent research has increasingly focused on distribution-level integrated energy systems, driven by the rapid growth of renewable generation, electrification of heating, and limited grid reinforcement capacity. In this context, distributed energy management architectures and decomposition-based optimisation algorithms have been reviewed in [17] to address scalability, privacy, and coordination challenges in integrated electricity and heat systems. In [18], a nonlinear formulation is employed to co-optimise integrated electricity and district heating systems, capturing the complex interactions and constraints inherent in both networks. The study in [19] presents an optimal scheduling algorithm that incorporates subsidy strategies to control heating system dispatch, focusing on economic incentives and policy-driven signals. A robust co-optimisation model combining a linear electrical network and a nonlinear gas network is developed in [20], demonstrating the benefits of integrated energy planning across vectors with different characteristics.

The operation of MES becomes more challenging with the addition of flexible loads and uncertain renewable sources. A literature overview on optimal power flow in MES and scheduling under uncertainty is discussed in the following subsections.

1.2.1 Optimal power flow in IEHS

As power systems evolve into multi-vector networks, the optimal power flow (OPF) problem must also expand to accommodate the physical and operational characteristics of electricity,

gas, and thermal systems. Future power grids and microgrids are expected to involve a variety of energy vectors on the generation side, such as solar, wind, heat, and gas. They also include controllable electricity and heat demands on the consumption side and energy storage devices [21]. While day-ahead scheduling is a well-studied problem in power systems, it becomes significantly more challenging in IEHS due to network interdependencies and the stochastic nature of multiple load types.

A substantial body of research has focused on solving the OPF problem for electrical networks using deterministic [22], stochastic [23–25], and heuristic methods such as particle swarm optimisation and genetic algorithms [26, 27]. Generation-reserve co-optimisation models have also been developed for integrated planning in [28]. For coupled electricity and gas networks, [29] proposes a hybrid dispatch framework, while robust optimisation techniques are adopted in [30, 31]. Furthermore, integrated electricity-heat-gas systems have been modelled using mixed-integer linear programming (MILP) in [32], providing tractable formulations for multi-energy dispatch problems. Most of these works adopt a linearised electrical network model based on DC optimal power flow (DC-OPF) or quadratic formulations. However, these simplifications can compromise accuracy in radial distribution systems, where non-convexities are more pronounced. To address this, a branch flow-based second-order conic programming (SOCP) model is proposed in [33, 34], which offers both accuracy and computational efficiency.

The State-of-the-art review in [35, 36] has highlighted the growing complexity of OPF formulations due to high renewable penetration, operational constraints, and uncertainty, as well as the increasing adoption of convex relaxation and data-driven methods to improve tractability and scalability. The modelling of DHS presents additional complexity due to the dual physical nature of thermal and hydraulic networks. A comprehensive steady-state model for DHS is presented in [37], while a dynamic equivalent model tailored for distributed IEHS is proposed in [38]. Other studies, such as [39], utilise data-driven approaches to approximate DHS behaviour. Simulation-based models are also explored for optimisation tasks in [40]. For solving steady-state thermal load flows, [41] introduces a Newton-Raphson-based method that improves

convergence speed.

1.2.2 Scheduling under uncertainty

The variability inherent to RES introduces significant uncertainty in system scheduling across multiple time scales. Robust optimisation approaches have seen significant advances in addressing this issue. In [42], a robust scheduling framework is developed for smart appliances and energy storage in residential settings, accounting for user behaviour uncertainty. Similarly, [43] presents a two-stage distributionally robust optimisation model for integrated energy systems with electricity-hydrogen storage. The first stage handles day-ahead planning, while the second refines the schedule using distributional robustness to adapt to intra-day deviations. Active power control (APC) and reactive power control are two commonly employed strategies for maintaining optimal voltage levels. APC has proven particularly effective in mitigating curtailment issues, as demonstrated in [44], where a droop-based control method is used to determine optimal curtailment levels. To account for decision-dependent uncertainty, an adaptive column-and-constraint generation algorithm is presented in [45], which offers robust generation scheduling under uncertain conditions.

Stochastic scheduling methods have also been extensively applied to model uncertainty in RES generation and load profiles. [46] proposes a stochastic multi-objective dynamic dispatch for CHP-based microgrids, integrating a system simulation module that captures wind, irradiance, and load uncertainties. In [47], a two-stage stochastic dynamic economic dispatch framework is introduced, where a stochastic decomposition method is used to manage wind uncertainty and improve generator pre-ramping decisions and reserve allocation. Another two-stage scheduling frameworks for community-level integrated energy systems, incorporating power-to-hydrogen and power-to-heat conversion is discussed in [48] to enhance operational flexibility under source–load uncertainty. Scenario-based stochastic formulation is proposed in [49], where wind uncertainty is incorporated into the economic dispatch problem using a backward scenario

reduction technique based on Euclidean distance. The model demonstrates how wind integration can be effectively handled in thermal generation systems while maintaining economic feasibility and grid stability.

Traditional deterministic and robust scheduling methods often struggle to balance economic efficiency with security constraints, especially in the face of forecast errors and volatile generation patterns. Among uncertainty-handling methods, chance-constrained optimisation has emerged as a powerful alternative to traditional stochastic and robust methods. The approach in [50] develops a chance-constrained economic dispatch (CCED) model that restricts risk exposure within a predefined confidence level. Another study, [51], formulates a joint dispatch model that simultaneously optimises wind curtailment and load shedding while managing reserve shortages and transmission congestion. These studies highlight the strengths of chance-constrained formulations in addressing feasibility issues and ensuring system security under uncertainty, especially when compared to deterministic or purely robust or stochastic strategies.

The reviewed literature highlights substantial progress in the modelling and optimisation of multi-energy systems, particularly in the coordinated operation of electrical and heating networks. However, most existing studies either focus on transmission-level planning, rely on simplified or decoupled network representations, or inadequately address operational uncertainty at the distribution level. Furthermore, while flexibility through storage and demand response is widely acknowledged, its practical integration into network-constrained IEHS scheduling remains limited. These observations motivate the development of co-optimisation frameworks that are computationally tractable, explicitly account for electrical and thermal network constraints, and are suitable for distribution-level operation under uncertainty.

1.3 Limitations of existing works

Many studies rely on simplified models of electrical and thermal networks to maintain computational tractability, particularly in large-scale or real-time contexts. These simplified approaches, including linear approximations and decoupled vector modelling, are often necessary trade-off's when full non-linear or hydraulic modelling is infeasible. However, they limit the ability to fully capture the network-level interactions, voltage and temperature constraints. A clear opportunity exists to develop modular, scalable co-optimisation frameworks that capture the operational essence of IEHS while remaining computationally efficient, particularly for practical implementations.

Although significant progress has been made in the field of MES optimisation, several challenges remain that limit the effectiveness and applicability of current approaches. Electrical systems are frequently modelled using linear approximations such as DC OPF, while thermal networks often rely on steady-state representations. These simplifications overlook critical non-linearities, voltage sensitivities, and dynamic thermal behaviours, which can result in inaccurate dispatch decisions or infeasible operational outcomes in real-world systems. Another notable shortcoming is the under representation of flexibility elements, such as demand-side response and energy storage. While flexibility is key to mitigating the variability of RES, many existing models treat loads as static and neglect their potential for temporal shifting. Consequently, the role of flexible loads and storage in enhancing system resilience and reducing curtailment is not fully realised. Here, flexibility refers to the ability of loads or storage systems to temporally shift energy consumption or production within predefined operational limits.

Additionally, the integration across energy vectors, particularly between electricity and heating, is often modelled in a loosely coupled or oversimplified manner. This approach fails to capture the operational inter-dependencies and mutual constraints of interconnected networks, which are essential for accurate co-optimisation. True multi-vector coordination, especially in integrated electricity and district heating systems, remains a technically and computationally

demanding task. Handling uncertainties in RES generation and load forecasting poses another major challenge. Although deterministic optimisation remains prevalent due to its simplicity, it cannot accommodate the inherent variability of modern energy systems. While some studies have employed robust or stochastic optimisation frameworks, these often require extensive scenario generation assumptions. Chance-constrained optimisation has emerged as a promising alternative but is still underutilised in IEHS applications.

Moreover, the growing complexity of MES models with their multiple vectors, temporal coupling, and operational constraints often results in highly dimensional and non-linear optimisation problems. Despite this, many studies overlook the computational burden and do not propose solution methods suitable for real-time or large-scale implementation. Curtailment control represents yet another underdeveloped area. Accurate estimation and active control strategies, such as adaptive curtailment and droop-based control, are still not widely integrated into IEHS scheduling frameworks, limiting their ability to prevent system violations like overvoltages or thermal overloads. Recent studies [52, 53] have investigated cyber–physical and data-driven scheduling for integrated energy systems. However, high complexity, data dependence, and challenges in enforcing network constraints limit their practical applicability.

Finally, many existing models do not fully reflect practical operational considerations. Factors such as equipment limitations, security constraints, comfort constraints in thermal systems, realistic forecasting errors, and computational complexities are frequently neglected. This disconnect between modelling assumptions and real-world constraints reduces the practical value and deployability of the proposed solutions.

1.4 Objectives and contributions

The core objective of this research is to develop a scalable and practical framework for the co-optimisation of IEHS, with a particular focus on managing uncertainties associated with

renewable energy sources and variable demand. This study aims to explore how coordinated scheduling across electrical and heating vectors can reduce curtailment, improve operational efficiency, and enhance the flexibility of the overall system under both deterministic and uncertain conditions.

To achieve this, the research is structured around two complementary studies. The first involves the formulation of a deterministic co-optimisation model for IEHS, focusing on the coordinated scheduling of generation units, storage systems, and flexible loads using simplified yet representative network approximations. The developed model is scalable and practical. The second study extends this model by incorporating uncertainty in renewable generation and load forecasts through a chance-constrained optimisation framework. Here, the model is designed to balance computational tractability with operational relevance, offering a basis for practical deployment and further enhancement.

The various research objectives and original contributions of this work are outlined below:

- A co-optimisation modelling framework for integrated electrical and district heating systems is presented, capturing the key operational inter-dependencies between the energy vectors.
- Deterministic and chance-constrained optimisation models are formulated to obtain optimal schedules for generation sources, curtailments, and flexible loads under both deterministic and uncertain forecast scenarios.
- A novel dynamic dispatch rule is proposed for real-time adjustment of active power curtailments and flexible load utilisation, enabling adaptive system response based on updated information.
- An efficient solution methodology based on scenario generation and reduction is adopted to solve the chance-constrained model, which increases the computational tractability of the method. The proposed frameworks are validated on benchmark test systems,

including the IEEE 15-bus and UKGDS 95-bus networks.

Together, these objectives aim to demonstrate the viability and benefits of coordinated scheduling in IEHS while addressing the practical challenges of uncertainty, computational complexity, and flexibility in real-world implementations.

1.4.1 Original contributions

Based on the research objectives set in the previous section, the following original scientific contributions are delivered from this research

1. **Proposed a linear co-optimisation strategy for electrical and district heating systems**

   This thesis proposed a linear co-optimisation framework for integrated electrical and district heating systems at the distribution level, where electric boilers and heaters act as interconnecting elements between the two networks. By jointly scheduling renewable generation, storage devices, and flexible electrical and thermal loads, the framework demonstrated how coordinated operation can reduce renewable energy curtailment and lower operational costs.

2. **Proposed a chance-constrained co-optimisation strategy for dynamic dispatch of electrical and district heating systems**

   This work developed a chance-constrained co-optimisation strategy to explicitly account for uncertainties in renewable generation and electrical and thermal load forecasts. The proposed formulation enables probabilistic enforcement of voltage and temperature constraints in distribution-level integrated electrical and district heating systems. A rule-based dynamic dispatch mechanism is introduced to obtain the renewable curtailment and electric boiler dispatch levels. The effectiveness of the approach is validated on bench-

mark distribution systems, demonstrating reduced voltage deviations and temperature violation constraints compared to deterministic scheduling.

1.4.2 Research dissemination

1. **Paper 1:** S. P. Polisetty et al., "Co-optimisation of Electrical and District Heating Networks: Bornholm case study," 2023 62nd IEEE Conference on Decision and Control (CDC), Singapore, Singapore, 2023, pp. 2549-2554, doi: 10.1109/CDC49753.2023.10383655.

   Abstract:

   With the growing energy demands, the interdependence among multiple energy domains is increasing rapidly. The optimal dispatch of the different energy sources, storage systems, and flexible loads in a multi-energy system is a challenging problem. This paper focuses on the co-optimisation of a multi-energy system consisting of electrical and district heating networks to address the challenge. The electric boilers and heaters act as interconnecting elements between the two systems. Utilising the available flexibilities in both systems, the co-optimisation focuses on energy management to achieve economical operation and reduction in renewable curtailment. The algorithm uses the day-ahead forecast of renewable generation as well as electrical and heating demands to determine the optimal schedule for the various generation, storage, and flexible loads in both systems. A case study based on the multi-energy system at Bornholm Island, Denmark, is presented in this paper. The results show a significant reduction in renewable power curtailment and a reduction in CO2 emissions achieved via the interconnected systems.

2. **Paper 2:** S. P. Polisetty, F. U. Nazir and B. C. Pal, "Chance Constrained Co-Optimization of Integrated Electrical and District Heating Networks," in IEEE Transactions on Power Systems, vol. 40, no. 4, pp. 3401-3412, July 2025, doi: 10.1109/TPWRS.2025.3527552.

   Abstract:

   Integrated electrical and heating systems (IEHS) are drawing huge attention because of their cost-effective and flexible operational capabilities. Optimal dispatch of renewable

units in an IEHS is challenging because of their intermittent and stochastic nature. Uncertainties in the renewable energy source (RES) forecast, electrical, and thermal loads can cause voltage and temperature violations, compromising the operational security of the system. In this paper, a rule-based dynamic dispatch is proposed to handle the increasing levels of uncertain RES and ensure the system's security. A chance-constrained (CC) co-optimisation algorithm considering the uncertain loads and RES is developed. In the proposed method, electric boiler power and curtailment of RES are dynamically dispatched to reduce operational costs and network losses. The developed method is tested on the IEEE 15 bus distribution system and the UK Generic Distribution System (UKGDS) 95 bus test system models. The results show that the proposed method significantly reduces the voltage deviations and temperature violations compared to the deterministic case.

3. **Poster:** S. P. Polisetty, F. U. Nazir and B. C. Pal, "Linear optimisation Model for Thermal Load Scheduling in Smart Buildings", *2022 IEEE Power & Energy Society General Meeting (PESGM)*, Denver, USA, 17-21 July 2022.

1.5 Organisation of the thesis

This thesis investigates the co-optimisation of IEHS with an emphasis on improving operational efficiency, reducing renewable energy curtailment, and managing the uncertainty associated with variable generation and demand. The work progresses from linear co-optimisation model to chance-constrained optimisation framework that integrate physical network constraints and uncertainties. Throughout this thesis, electrical power is expressed in MW, thermal power in MW, voltages in per unit ($p.u.$), and temperatures in degrees Celsius (^oC), unless stated otherwise. The remainder of the thesis is organised into the following chapters:

- **Chapter 2** introduces the initial co-optimisation framework developed as part of the

first phase of this research. This chapter presents a linear programming-based model for the coordinated scheduling of generation sources, storage systems, and flexible electrical and thermal loads. Interconnection between the two networks is achieved through electric boilers and heaters, facilitating sector coupling and energy balancing. The model is validated through a case study based on the Bornholm Island energy system in Denmark, demonstrating improvements in renewable energy utilisation and reductions in both operational cost and CO_2 emissions. This chapter also presents simulation results of a few practical scenarios.

- **Chapter 3** significantly extends the modelling complexity by introducing detailed physical representations of both the electrical and district heating networks. The electrical system is modelled using a second-order conic (SOCP) formulation of the OPF problem, allowing accurate modelling of voltage constraints in radial distribution networks. The district heating network is modelled using a steady-state thermal-hydraulic framework, considering mass flow rates and temperature constraints. This chapter first presents a deterministic optimisation formulation for the integrated system, and then transitions to a chance-constrained optimisation approach to account for uncertainties in renewable energy forecasts and load demand. Additionally, a scenario generation and reduction methodology is incorporated to improve the tractability of the chance-constrained model without sacrificing solution quality. This chapter lays the theoretical and methodological foundation for uncertainty-aware co-optimisation in IEHS.

- **Chapter 4** presents extensive numerical simulations for both the deterministic and chance-constrained optimisation models. The test systems include the IEEE 15-bus radial distribution network and the UKGDS 95-bus network. Multiple uncertainty scenarios for RES generation and load profiles are generated and analysed. The simulation results highlight the impact of integrated energy system coordination on voltage regulation, temperature compliance in heating networks, renewable energy curtailment, and total system costs. A detailed comparison between the deterministic and chance-constrained models

is provided to demonstrate the value of probabilistic approaches in ensuring secure and economic operation under uncertainty.

- **Chapter 5** summarises the key findings and conclusions drawn from the presented work. The chapter also outlines the potential future directions for research, including the integration of real-time control mechanisms, coupling with other energy networks, the inclusion of dynamic thermal models, and the use of data-driven or machine learning-based forecasting and decision support tools.

Chapter 2

Scheduling of integrated electrical and heating systems

This chapter presents a linear co-optimisation framework for the day-ahead scheduling of an islanded IEHS. The primary goal is to determine the optimal dispatch of conventional and renewable generators, flexible loads, and storage units, while minimising operational costs and renewable curtailment. A test system based on the Bornholm Island energy infrastructure is used to demonstrate the modelling approach and its benefits.

The integrated model captures the operational interdependencies between an electrical power system (EPS) and a district heating system (DHS). The EPS comprises conventional generators, solar PV, wind sources, inflexible and flexible electrical loads, which include central electric boilers and household electrical heaters. The DHS includes conventional boilers, central electric boilers, and hot water tanks (HWTs) serving various end-users such as households, schools, and community swimming pools. Electric heaters in households and electric boilers at the DHS plant form the coupling elements between the two domains, enabling energy flexibility across sectors. These interconnecting devices are modelled as flexible electrical loads, while schools and pools serve as flexible thermal loads on the DHS side. These flexible demands are time-shiftable but

constrained by hourly consumption limits.

2.1 Electric power system

The EPS consists of conventional sources and renewable sources which will balance the inflexible and flexible electrical demands of the system. The power balance equation for EPS is given by

$$P_t^{CG} + P_t^{RES} = D_t^B + D_t^{FL} + P_t^{RES_curt} \tag{2.1}$$

where P_t^{CG} is the net conventional generation power, P_t^{RES} is the net power from renewable sources. D_t^B is the base electrical demand of the entire island, D_t^{FL} is the flexible electrical demand and $P_t^{RES_curt}$ is the curtailed renewable power.

The inflexible demand D_t^B is the forecasted base demand of the complete island, and D_t^{FL} is the flexible demand which will be determined by the co-optimisation. $P_t^{RES_curt}$ is the curtailed renewable power, which will always be a positive quantity. The flexible demand includes the electric boilers demand, D_t^{EB} at the DHS plant, and the net electric heaters demand, D_t^H at the household level which is given by

$$D_t^{FL} = D_t^{EB} + D_t^H \tag{2.2}$$

Conventional generators are associated with constraints representing their capacity limits, while flexible loads are bounded by limits on their consumption at any given hour. The subscripts min and max denote the minimum and maximum limits of each variable, respectively, as expressed by

$$\begin{aligned} P_{\min}^{CG} \leq P_t^{CG} \leq P_{\max}^{CG}, \\ D_{\min}^{EB} \leq D_t^{EB} \leq D_{\max}^{EB}, \\ D_{\min}^{H} \leq D_t^{H} \leq D_{\max}^{H}. \end{aligned} \tag{2.3}$$

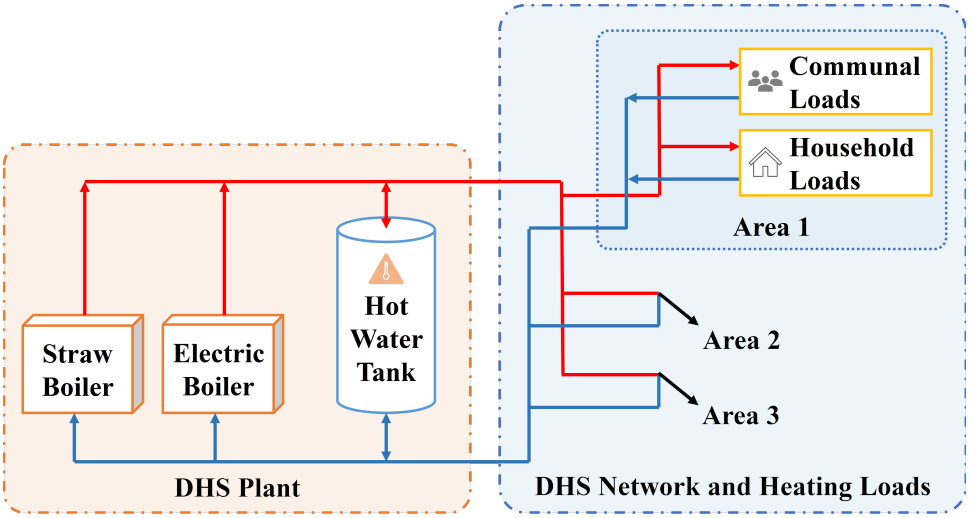


Figure 2.1: DHS at Bornholm consisting of heating plant and consumers

The forecast of PV and wind generation and the forecasted base demand are parameters that are inputs to the optimisation. The rest of the variables, which include the generation from conventional sources and the flexible demand and curtailment, are optimised by the co-optimisation algorithm.

2.2 District heating system

The DHS consists of a hot water supply plant, flexible communal loads, and inflexible household loads connected as shown in Fig. 2.1. The DHS plant generates heat power, H_t^S, from conventional sources and also from electric boilers, H_t^{EB}, which will be utilised to heat the water and cater to the inflexible demand, H_t^B, and flexible demand, H_t^{FL}. The hot water tank (HWT) is used to store or retrieve heat energy and constitutes the flexibility to serve the demand at a later stage during the period of high fuel cost or renewable intermittencies. $H_t^{HWT_out}$ and $H_t^{HWT_in}$ represent the output and input heat power of the HWT. At the household level, electric heaters will also heat the hot water. The aggregated net heat power of the electric heaters is denoted by H_t^H. All DHS components and flexibility resources are coordinated within a centralised optimisation framework, and the resulting scheduling problem is formulated for day-ahead scheduling

and solved as a mixed-integer linear programming (MILP) problem.

The heat power balance equation governing the DHS plant and the consumer loads is expressed as

$$H_t^S + H_t^{EB} + H_t^H + H_t^{HWT_out} - H_t^{HWT_in} = H_t^B + H_t^{FL} \tag{2.4}$$

The heat energy stored in HWT is denoted by E_t^{HWT}. The HWT is constrained by minimum and maximum storage limits, while its energy evolution is governed by the charging and discharging power over the time step Δt, as expressed by

$$\begin{aligned} E_t^{HWT} &= E_0^{HWT} + (H_{HWT_{\text{in}}} - H_{HWT_{\text{out}}})\,\Delta t, \quad t = 1, \\ E_t^{HWT} &= E_{t-1}^{HWT} + (H_{HWT_{\text{in}}} - H_{HWT_{\text{out}}})\,\Delta t, \quad t \geq 2, \\ E_{\min}^{HWT} &\leq E_t^{HWT} \leq E_{\max}^{HWT}. \end{aligned} \tag{2.5}$$

The heat generated from the conventional heat source is limited by its rated capacity. In addition, the HWT is constrained by maximum charging and discharging rates, and it must be ensured that the HWT operates either in charging or discharging mode at any given time. These operational constraints are expressed as

$$\begin{aligned} H_{\min}^S \leq H_t^S \leq H_{\max}^S, \\ H_{\min}^{HWT} x_t^{HWT_{\text{out}}} \leq H_t^{HWT_{\text{out}}} \leq H_{\max}^{HWT} x_t^{HWT_{\text{out}}}, \\ H_{\min}^{HWT} x_t^{HWT_{\text{in}}} \leq H_t^{HWT_{\text{in}}} \leq H_{\max}^{HWT} x_t^{HWT_{\text{in}}}, \\ x_t^{HWT_{\text{out}}} + x_t^{HWT_{\text{in}}} \leq 1, \end{aligned} \tag{2.6}$$

where $x_t^{HWT_{\text{out}}}$ and $x_t^{HWT_{\text{in}}}$ are binary variables indicating the discharging and charging states of the HWT, respectively. These variables are part of the optimisation and solved using the MILP formulation.

2.3 Coupling strategy and independent optimisation cases

The EPS and DHS are modelled as two independent energy networks, each governed by its own balance equations and operational constraints. In the proposed co-optimisation framework, these systems are integrated through electric boilers at the heating plant and electric heaters at the household level as shown in Fig. 2.2, which act as coupling elements between the two domains. These devices appear as flexible electrical loads in the EPS and as controllable heat generation units in the DHS. The interaction between the networks is enforced through linear conversion constraints that relate electrical power consumption to thermal energy output using fixed efficiencies. The relationship between the electrical power and the produced thermal power can be expressed as

$$\begin{aligned} H_t^{EB} &= \eta^{EB} D_t^{EB}, \\ H_t^{H} &= \eta^{H} D_t^{H} \end{aligned} \tag{2.7}$$

where η^{EB} and η^{H} denote the conversion efficiencies of the electric boiler and the electric heater, respectively. D_t^{EB} and D_t^{H} are the electrical demands of electrical boiler and electric heater respectively.

For comparison purposes, independent optimisation cases are also considered. In the EPS-only case, the electrical system is optimised without interaction with the heating network, and all thermal demand is excluded. In the DHS-only case, the heating system is optimised independently, with all thermal demand supplied by conventional heat sources and thermal storage, and without access to electricity-driven heating. In both independent cases, the same demand and generation forecasts and technical limits are used as in the co-optimised case. The performance of the independent and co-optimised frameworks is evaluated using consistent metrics, including renewable energy curtailment, operational cost, fuel consumption, and CO_2 emissions.

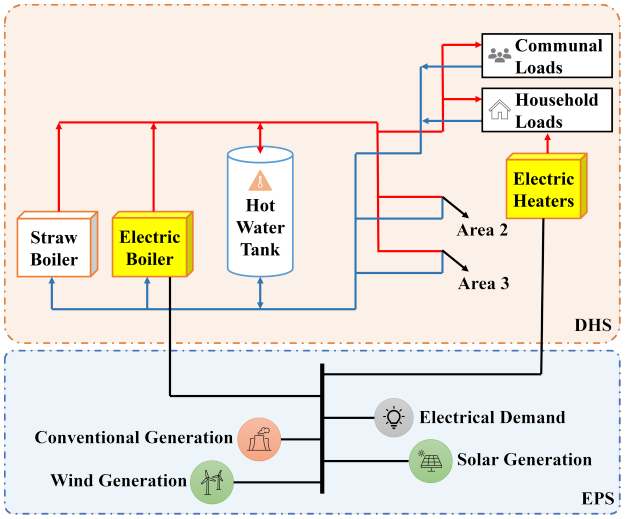


Figure 2.2: Interconnection between EPS and DHS at Bornholm

2.4 Linear co-optimisation of IEHS systems

The main objective of the co-optimisation algorithm is to utilise the flexibility from the DHS system in the EPS to avoid renewable curtailment and reduce the use of conventional generation and boilers. This is achieved by utilising the electric boilers at the DHS plant to cater to the real-time heating demand and store the excess heat energy in the hot water tank. This reduces the use of conventional boilers of the DHS plant and maximises the renewable utilisation of the island. The co-optimisation will make sure that the electric boilers are utilised during the period of peak renewable generation. The HWT will ensure to store hot water when excess renewable power is available and discharge during the low renewable period and high heat demand periods. The heating demand can also be catered by the electric heater at the consumer premise which will help in further utilisation of renewable energy.

2.4.1 Cost function

The cost function reflects the objectives of co-optimisation which are low operation cost, low renewable curtailment, and maximum utilisation of HWT. The objective function, F consists

of operating cost, C_O and penalty cost, C_P which can be wrriten as

$$F = C_O + C_P \tag{2.8}$$

The operational cost includes the cost of generation from various conventional generators in EPS and the conventional heat sources of DHS. C_O can be expressed as

$$C_O = \sum_{t=1}^{24} (c_{CG} P_t^{CG} + c_H H_t^s) \tag{2.9}$$

where c_{CG} represents the cost for electrical generation from various conventional generations like biogas, CHP, and fossil fuel power plants, and c_H is the cost of heat energy generated using the conventional heat sources.

The co-optimisation tries to avoid any renewable curtailment, and a penalty price, p_{RES}, is assigned for the curtailed power to minimise total penalty. The penalty associated with the renewable curtailment is expressed as

$$C_p = \sum_{t=1}^{24} (p_{RES} P_t^{RES_curt}) \tag{2.10}$$

The optimisation algorithm will minimise the cost function F subject to various constraints associated with the EPS and DHS. The entire co-optimisation formulation to solve a day-ahead scheduling problem can be described as

$$\begin{aligned} \min_{P_t^{CG}, H_t^s, P_t^{RES_curt}, x_t} \quad & F \\ \text{subject to} \quad & (2.1) - (2.7) \end{aligned} \tag{2.11}$$

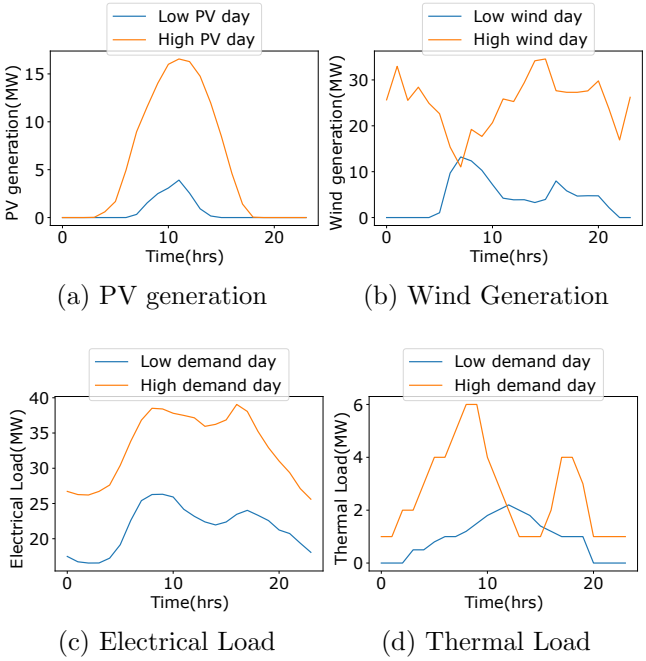
2.5 Simulation results

The electrical sources considered for the simulation analysis are PV, wind, and conventional generation from CHP, Biomass, and fossil fuel generators on the island of Bornholm. For analysis purposes, a single price for conventional generation sources is considered here. The electrical demand includes the total fixed electrical load of the island and flexible electric load power comprising electric boilers at the DHS plant and electric heaters at households. The DHS plant is equipped with conventional and electrical boilers as shown in Fig. 2.1. The heating demand of the DHS network consists of the forecasted base heating demand of households and the flexible communal heating demand.

The typical renewable generation and electrical demand profiles for the island are selected from historical data available in [54]. The curtailment cost is the penalty cost for curtailing renewable power. The power system operator should define this value depending on any agreements with RES plants, the energy market, and other policies. The PV generation, wind generation, and load profile of the island for two typical days are shown in Figure 2.3. The days are selected to take into consideration the two extreme cases of generation or load. Since the historical data on the heating demand of the DHS plant is not available, a fictitious variation is used for the simulation analysis, which is shown in Fig. 2.3.

Various parameters for the simulation studies are listed in Table 2.1. It is noted that the electrical power system considered in the simulations has a significantly higher installed capacity (approximately 96 MW) compared to the district heating system, which operates in the range of 4 MW. This disparity reflects the realistic sizing of energy infrastructures, where electrical systems are designed to serve large-scale, system-wide demand, while district heating systems are typically localised and sized according to thermal requirements of specific consumer clusters. The aim of the proposed co-optimisation framework is not to match system capacities but to exploit their operational interdependencies.

In case of a high-demand day, it is assumed that the household heating loads will be higher



(a) PV generation (b) Wind Generation

(c) Electrical Load (d) Thermal Load

Figure 2.3: Typical generation and load profiles for a day at Bornholm

during the morning and evening time periods. A typical bell curve is considered in the case of a low-demand day. The communal loads act as flexible loads for the heating system. These flexible loads allow time-shifting and try to reduce the total operating cost. The communal loads are mostly catered by HWT or EB instead of a conventional heat source, which increases the operating cost. Based on the different generation and demand profiles, three test cases are considered to analyze the outcome of the co-optimisation algorithm. A comparison of co-optimisation and individual system optimisation is also presented here.

Case 1: High RES generation and high demand In this scenario, high power generation from renewable sources and high fixed demand in both systems is considered. Generally, high renewable generation and high demand might not occur on the same day, but this fictitious case is considered to demonstrate the savings with the algorithm. The generation and demand profiles are shown in Fig. 2.3. The result of the co-optimisation for this case is illustrated in Fig. 2.4.

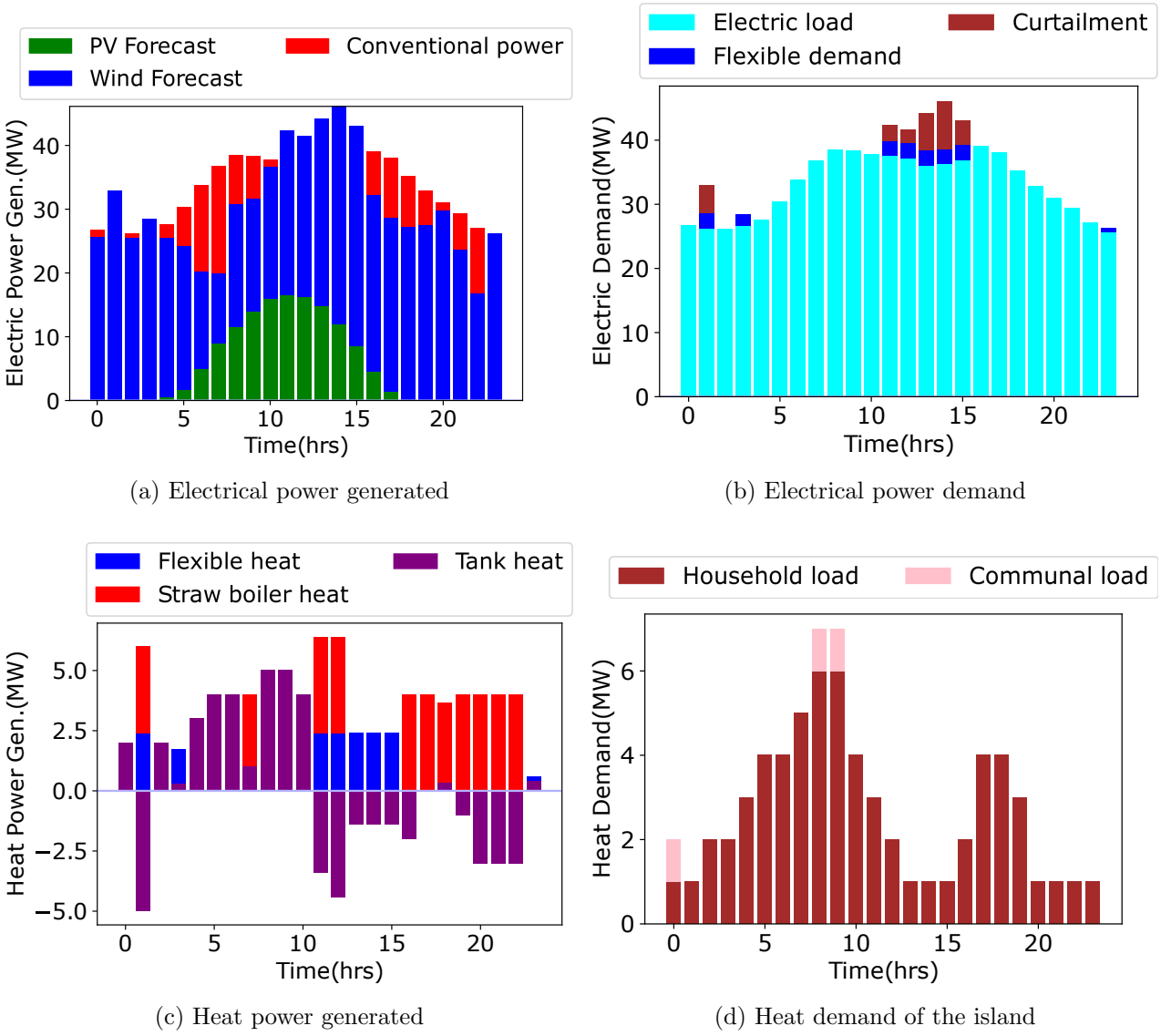
During the time instants when the demand is more than the renewable generation, conventional

Table 2.1: Simulation parameters

Parameter	**Value**	**Parameter**	**Value**
P^{CG}_{min}	0 MW	P^{CG}_{max}	96 MW
H^{S}_{min}	0 MW	H^{S}_{max}	4 MW
D^{EB}_{min}	0 MW	D^{EB}_{max}	2.2 MW
D^{H}_{min}	0 MW	D^{H}_{max}	0.2 MW
H^{HWT}_{min}	0 MW	H^{HWT}_{max}	5 MW
E^{HWT}_{min}	0 MWh	E^{HWT}_{max}	80 MWh
H^{FL}	3 MW	p_{RES}	537.85 €/MW
c_{CG}	141.2 €/MW	c_{H}	26.89 €/MW

generators are used to generate additional power. For instants when the demand is less than the renewable generation, the excess power is used to cater to the flexible demand comprising of the electric boilers and electric heaters of the DHS. The flexible electric power in this scenario is as shown in Fig. 2.4b. In case the flexible power reaches the maximum limit, the excess renewable generation is curtailed. The flexible electric power is utilised to heat the hot water at DHS and/or at households using the heaters.

Conventional boilers are operated in coordination with electric boilers to meet the heat demand of the island. The HWT charging and discharging is as shown in Fig. 2.4c. It can be observed that hot water is being stored during the hours when renewable power is curtailed i.e., during the excess renewable generation period. The time-shifting property of communal loads allows the load to be shifted to times when conventional boilers are not operating and also during high RES availability times. It can be seen in Fig. 2.4d that the communal load is being catered by HWT instead of being catered by conventional boilers. The use of a co-optimisation algorithm and the usage of electrical boilers during the instants of excess RES generation has resulted in the reduction of RES curtailment by 16.73 MWh. The use of electric boilers in the DHS plant has also reduced the usage of the conventional boiler. The comparison of optimising both the systems individually, i.e., independent case and co-optimisation, is summarised in Table 2.2.



(a) Electrical power generated

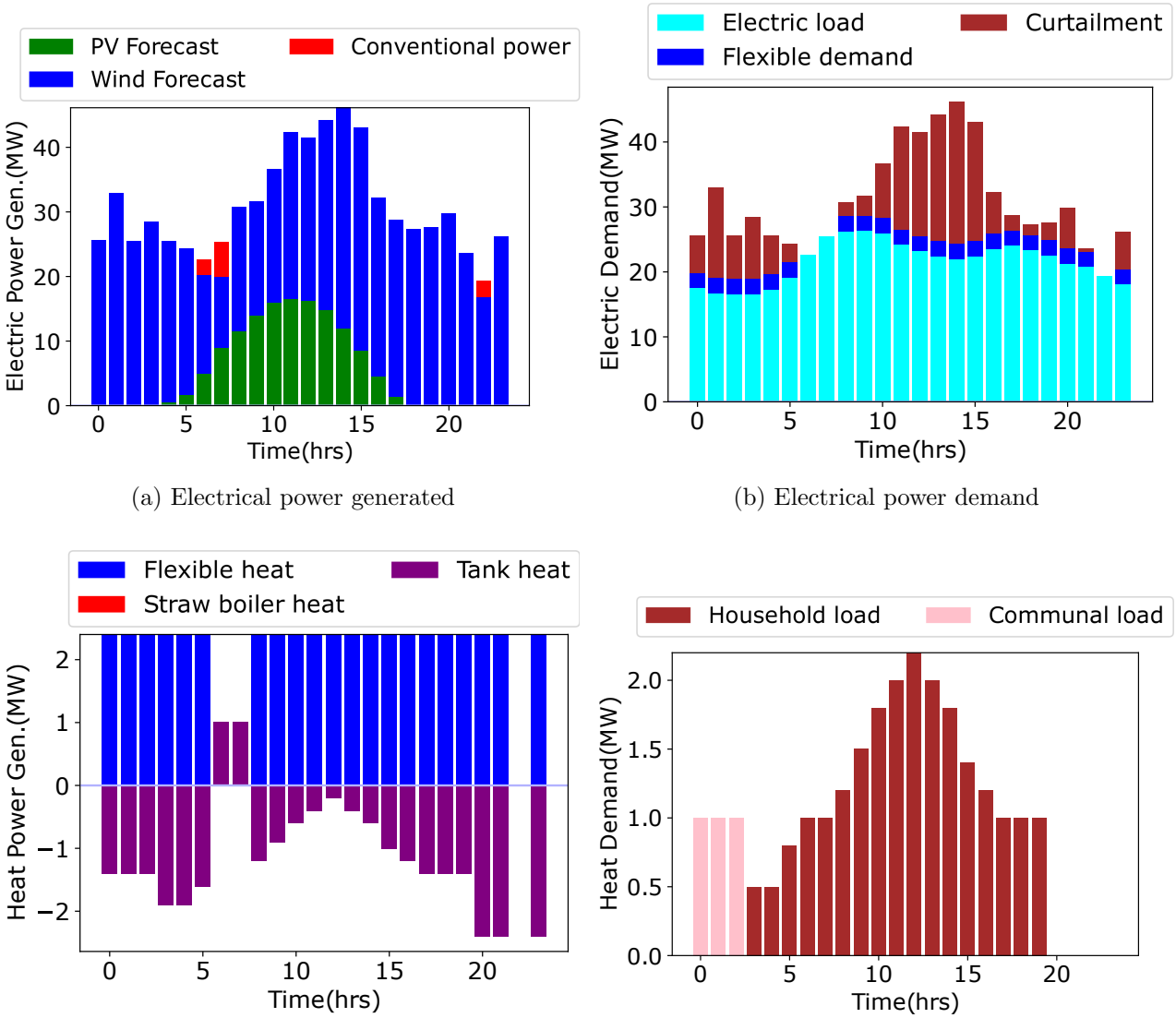
(b) Electrical power demand

(c) Heat power generated

(d) Heat demand of the island

Figure 2.4: Total electrical and heat power generation and demand in the island for case 1

Case 2: High RES generation and low demand In this scenario, high power generation from renewable sources and low fixed demand in both systems are considered. The result of the co-optimisation for this case is illustrated in Fig. 2.5. As the electrical demand in the EPS is low, as shown in Fig. 2.5b, compared to the RES generation in Fig. 2.5a, there is an excess of generation. The excess RES generation is utilised by the flexible boilers and heaters by turning them on at maximum capacity, thereby reducing the renewable curtailment. The electric boilers acting as the load of the EPS system during hours of excess RES are shown as the flexible power in Fig. 2.5b. The heat generated from the electric boilers is either used for



(a) Electrical power generated

(b) Electrical power demand

(c) Heat power generated

(d) Heat demand of the island

Figure 2.5: Total electrical and heat power generation and demand in the island for case 2

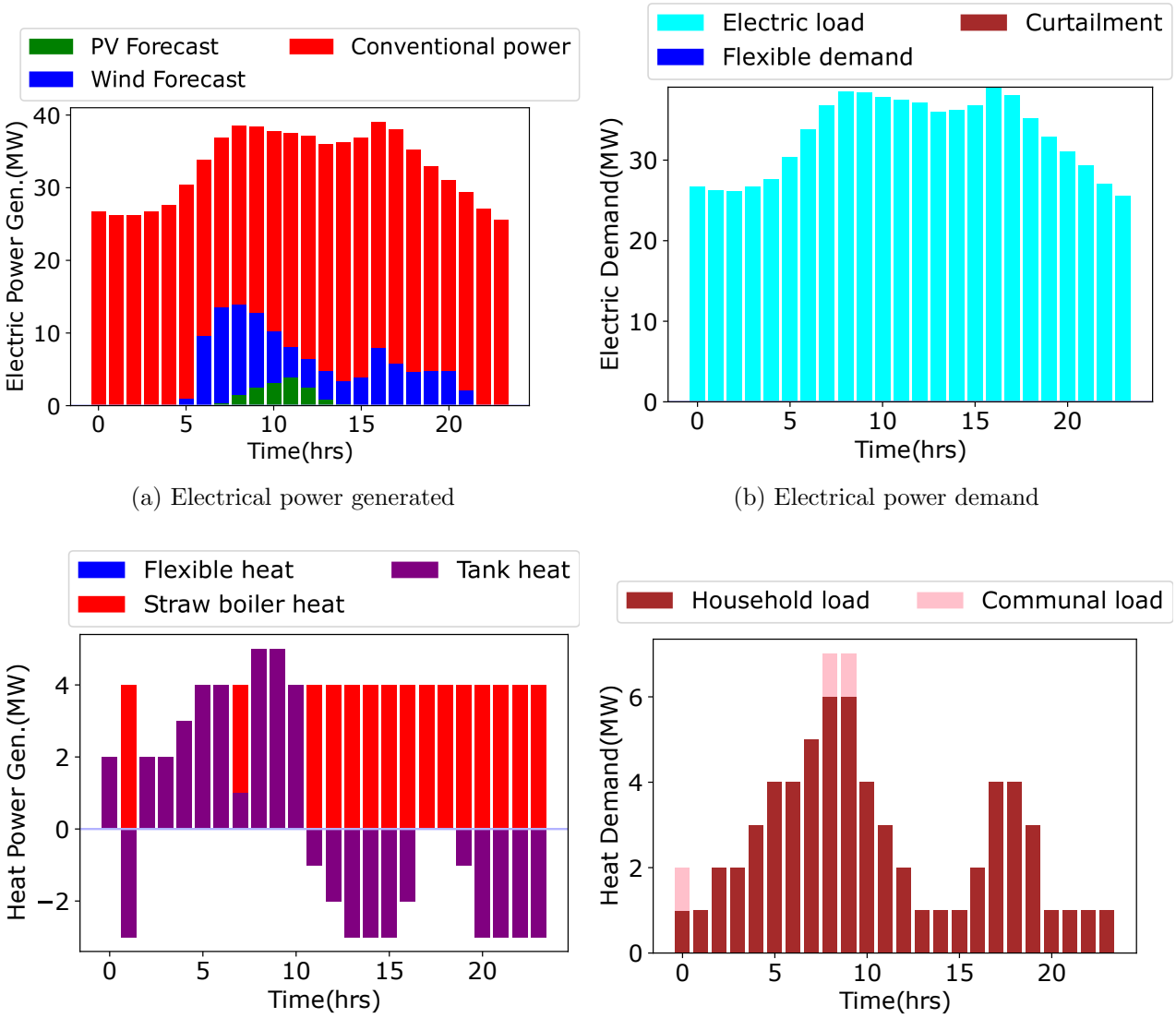
catering to the heat demand of the island (both household and communal) or to charge the hot water tank. In Fig. 2.5c, the flexible heat is at the maximum capacity, and the hot water tank is getting charged during most of the hours indicated as a negative value in Fig. 2.5.

During the period of renewable intermittencies, the electrical demand is catered to by conventional generators. The heat generated by the electrical boiler is used to cater to the household and communal loads as well as to charge the hot water tank. The hot water tank is charged within the limits of operation to utilise the RES generation. The excess heat energy stored in

the hot water tank can be used during the subsequent scheduled hours, thereby reducing the conventional boiler usage. It can be seen in Fig. 2.5d that the communal loads are shifted to the time when high RES is available. This time-shifting property helps in reducing the overall operating cost of the system. The comparison of optimising both the systems individually and performing co-optimising is summarised in Table 2.3. The co-optimisation has resulted in the reduction of curtailment by 50.4 MWh which is a 22.4% reduction. Here, the electric boiler is not utilised when conventional electric power is being utilised. Also, the conventional boiler is never turned on in this scenario using the co-optimisation method and CO_2 emissions are zero.

Case 3: Low RES generation and high demand This scenario considers a case in which the generation from renewable sources is low and the demand in both systems is high. The typical low PV day and low wind day profiles are considered for PV and wind generation. The typical high-demand profile is considered for electrical and heat loads, which are shown in Fig. 2.3.

The result of the co-optimisation is illustrated in Fig. 2.6. As the electrical demand is not able to be met by the RES, the conventional generation units are used to cater to the demand. Since there is no excess generation from EPS, the DHS plant relies on the conventional boiler to generate the heat power to cater to the various heating demands. The electric boiler does not take part in the DHS operation in this case. The communal loads are catered by HWT which are charged by conventional boiler. As we cannot use any RES here, the time-shifting loads cannot provide much cost savings in this case. In this scenario, flexible elements are not utilised by EPS and results in identical operational outcomes for both independent optimisation and co-optimisation.



(a) Electrical power generated

(b) Electrical power demand

(c) Heat power generated

(d) Heat demand of the island

Figure 2.6: Total electrical and heat power generation and demand in the island for case 3

2.6 Conclusions

A co-optimisation algorithm for the optimal dispatch of generation sources, storage, and flexible loads in IEHS is presented in this chapter. Day-ahead forecasts of renewable generation as well as demands of different energy domains are the inputs for this algorithm. The numerical results for the Bornholm island scenario, consisting of electrical and district heating networks, were presented. The obtained day-ahead optimal schedules show a significant reduction in renewable curtailment and efficient utilisation of electric boilers and thermal storage. This is

Table 2.2: Comparison of independent optimisation and co-optimisation for case 1

Case	Case 1		
	Independent	Co-optimisation	Change
Renewable curtailment	42.7 MWh	25.9 MWh	39.2%
Fuel cost of conventional boiler (EUR)	1146	846	26.2%
CO_2 emissions from conventional boiler (ton)	23.04	17.01	6.03
Energy gain of the hot water tank (MWh)	0	0	

mainly achieved by proper time-shifting of the flexible loads.

The three simulation cases highlight the impact of renewable availability and demand levels on the effectiveness of co-optimisation. In Cases 1 and 2, where surplus renewable generation is present, coordinated operation of the electrical and heating systems enables effective utilisation of electric boilers and thermal storage, resulting in significant reductions in renewable curtailment, operating cost, and CO_2 emissions. In contrast, Case 3 represents a low-renewable scenario in which the absence of surplus renewable generation limits the activation of flexible elements, resulting in identical operational outcomes for both independent optimisation and co-optimisation. The co-optimisation resulted in an overall reduction of the operating cost of both systems and a reduction in CO_2 emissions.

Table 2.3: Comparison of independent optimisation and co-optimisation for case 2

Case	Case 2		
	Independent	Co-optimisation	Change
Renewable curtailment	224.8 MWh	174.5 MWh	22.4%
Fuel cost of conventional boiler (EUR)	902	0	100%
CO_2 emissions from conventional boiler (ton)	18.14	0	18.14
Energy gain of the hot water tank (MWh)	0	23	23

Chapter 3

Chance-constrained co-optimisation of IEHS

3.1 Introduction

As discussed in Chapter 1, the growing penetration of RES has introduced a new dimension of uncertainty and variability in both electrical and thermal energy networks. These uncertainties, driven by weather-dependent generation and fluctuating load demands, pose a critical challenge to the economic operation of IES. As deterministic optimisation frameworks struggle to handle the increasing levels of stochasticity, there is a growing need for advanced optimisation techniques that incorporate risk-aware decision-making.

Chance-constrained optimisation has emerged as a powerful method for addressing uncertainties in multi-energy systems. Unlike robust or purely stochastic models, chance-constrained formulations enable system operators to maintain the feasibility of operational constraints with a high probability. In the context of IEHS, such probabilistic formulations allow for more realistic and flexible scheduling of controllable resources, particularly in scenarios involving high RES penetration.

This chapter presents a novel chance-constrained co-optimisation framework that simultaneously models the electrical and district heating networks under uncertainty. The proposed method builds upon a base case deterministic formulation and extends it using a scenario-based approach that captures the probabilistic nature of load and RES forecasts. Electric boilers serve as the coupling elements between the two networks, enabling flexibility through dynamic dispatch. Monte Carlo simulations are employed to generate a diverse set of scenarios that reflect realistic variations in system inputs, while scenario reduction techniques ensure computational tractability.

The chapter is structured as follows. First, the deterministic formulation of the co-optimisation problem is revisited, highlighting the control variables and system constraints. Next, the mathematical formulation of the chance-constrained model is developed, including the scenario-based implementation strategy. The chapter then details the use of linear dispatch rules for real-time flexibility, followed by a discussion of the submodular scenario reduction (SSR) methodology. Finally, the complete solution algorithm is outlined, demonstrating how the proposed framework ensures operational feasibility under uncertainty while minimising system costs.

3.2 Electrical and heating system modelling

In this section, the modelling of electrical and heating systems is discussed. Two widely used modelling methods for radial distribution systems are the branch flow method and the bus injection method. A branch flow model with convex relaxations [33] is adopted in this work as it has multiple advantages, like solution accuracy and better computational speed. Constant flow variable temperature method is adopted here for district heating systems to obtain the node temperatures for the required optimisation model.

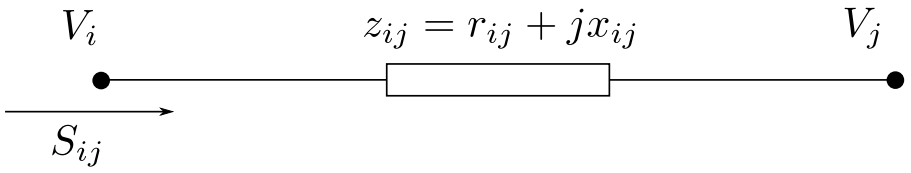


Figure 3.1: Line model in a distribution system

3.2.1 Electrical power flow modelling

Let N_E denote the nodes in the electrical network indexed by i = 0,1,.....n and B_E denote all the branches/links denoted by (i, j) if it points from node i to node j. Then the connected graph takes the form, $G = (N, E)$. For a radial network, if the number of nodes is n+1, then the number of branches is n. The voltage at node i is represented by V_i and the complex power flowing from node i to j is represented by S_{ij} as shown in Fig. 3.1. Also, the impedance of the line ij is represented by $z_{ij} = r_{ij} + jx_{ij}$.

The branch flow equations include the voltage drop equation of each branch, complex power flow in each branch and power balance at each node. The voltage drop equation of each branch can be written as,

$$V_i - V_j = z_{ij} I_{ij}, \ \forall (i, j) \in B_E \tag{3.1}$$

The branch complex power flow can be defined as

$$S_{ij} = V_j I_{ij}^*, \ \forall (i, j) \in B_E \tag{3.2}$$

The power balance at each node j can be written as

$$\sum_{k:j\to k} S_{jk} - \sum_{i:i\to j} (S_{ij} - z_{ij}|I_{ij}|^2) + y_j^*|V_j|^2 = s_j, \forall j \in N_E \tag{3.3}$$

where s_j is the net complex load power on bus j and y_j is the shunt admittance from bus j to ground. Equations (3.1)–(3.3) represent the branch flow equations. Here, the notation $j \to k$ represents the branch from the upstream node j connected to downstream node k. Let $\mathbb{X}$(s) be

the set of all the branch flow solutions for a given s, then we can write:

$$\mathbb{X}(s) := \{x := (S, I, V, s_0) - x \text{ solves (3.1)-(3.3) given } s\} \tag{3.4}$$

For the relaxed model, we can define $l_{ij} = |I_{ij}|^2$ and $v_i = |V_i|^2$. Separating the real and imaginary parts of (3.1)-(3.3) will give the following,

$$p_j = \sum_{k:j\to k} P_{jk} - \sum_{i:i\to j}(P_{ij} - r_{ij}l_{ij}) + g_j v_j, \forall j \in N_E \tag{3.5}$$

$$q_j = \sum_{k:j\to k} Q_{jk} - \sum_{i:i\to j}(Q_{ij} - x_{ij}l_{ij}) + b_j v_j, \forall j \in N_E \tag{3.6}$$

$$v_j = v_i - 2(r_{ij}P_{ij} + x_{ij}Q_{ij}) + (r_{ij}^2 + x_{ij}^2)l_{ij}, \forall (i,j) \in B_E \tag{3.7}$$

$$v_i l_{ij} = P_{ij}^2 + Q_{ij}^2, \forall (i,j) \in B_E \tag{3.8}$$

Here, p_i and q_i represent the net real and reactive power consumption at node i. P_{ij} and Q_{ij} represent the real and reactive power flowing in the line ij. Equation (3.8) is a non-convex second-order equation. This can be relaxed to an inequality equation 3.9 and still obtain an exact solution for radial systems under mild assumptions [33]. This relaxation is tight and holds till we maintain a convex objective function, which will be discussed in section 3.3. By relaxing the equality constraint, a convex optimal power flow model can be obtained as

$$l_{ij} \leq \frac{P_{ij}^2 + Q_{ij}^2}{v_i} \tag{3.9}$$

Finally, (3.5–3.7),(3.9) represents the complete convex radial power flow equations. For the buses connected with RES, $p_j = p_{lj} - p_{gj}$. Here, the renewable generation is a dynamic dispatch variable whose dispatch power is identified after curtailing the optimal amount of active power. Thus, $p_{gj} = p_{gj}^f - p_{cj}^d$. Also, for the buses connected with power-transferring devices like EBs, the load power can be expressed as $p_{lj} = p_{lj}^f - p_{ebj}^d$. For the optimal power flow (OPF), RES active power and electrical boiler power are also optimisation variables.

3.2.2 Thermal power flow modelling

According to [55, 56], the DHS network can be divided into two separate parts, supply and return networks. Each network have the same physical and geometric properties. Load management studies state that DHS has supply temperature, return temperature, load flow rate, and differential pressure as variables [57]. Also, the utility supplies the hot water to the consumers and thus controls the supply temperature and differential pressure. Meanwhile, the consumption will depend on the end users, which will determine the return temperature and flow rate. Different load control methodologies include constant flow control, variable flow control, demand-based and weather-compensated control, etc., These control methods extract maximum heat from the supplied hot water and maintain the low return temperatures [55]. Also, most of the modern controllers use constant return temperature control [56]. By exploiting this mode of operation, we are able to simplify the optimisation framework and achieve the desired control by optimising the supply temperature alone. In the proposed method, DHS is modelled as a constant flow and variable temperature (CFVT) network, which is a linear and pragmatic modelling assumption.

The district heating system comprises hydraulic and thermal sub-systems. The hydraulic model determines mass flow rates in each pipe, while the thermal system decides the temperature at each node of the sending and receiving networks. As mentioned, the DHS is controlled using the CFVT method. Thus, the hydraulic system is fixed, and the thermal circuit alone is controlled. Fig. 3.2 represents a pipe model of the district heating system. Here, T_i denotes the temperature at node i of the supply network. The variables T_i^{p+} and T_i^{p-} represent the outflow and inflow temperatures of supply pipe i, respectively. The term $\dot{m}_i$ denotes the net mass flow rate consumed at node i, while $\dot{m}_i^p$ represents the mass flow rate in supply pipe i.

In this work, the hydraulic sub-system is not explicitly optimised. Instead, pressure drops and pump dynamics are implicitly accounted for by assuming a fixed mass flow profile obtained from the CFVT operating strategy. This assumption reflects common operational practice in

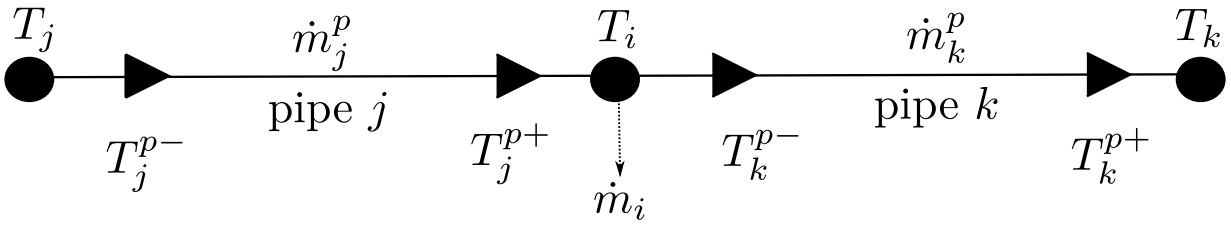


Figure 3.2: Pipes representation in district heating system

modern DHS, where flow rates are regulated at the supervisory level and remain quasi-static over the optimisation horizon. As a result, pressure-related constraints do not appear explicitly in the formulation, and the analysis focuses on the thermal feasibility of the network under given flow conditions.

The adopted CFVT modelling approach introduces several simplifying assumptions. First, mass flow rates are assumed to be known and constant, which neglects short-term hydraulic transients and pump control actions. Second, heat losses along the pipes are modelled using an exponential decay function with constant parameters, assuming uniform pipe characteristics and ambient conditions. Third, return network temperatures are treated as fixed, which is consistent with constant return temperature control strategies but may not capture user-side variability in extreme operating conditions. These assumptions allow the DHS model to remain linear and computationally tractable while preserving the dominant thermal behaviour relevant for co-optimisation.

The heat consumption at node i can be written as

$$\Phi_i = c_p \dot{m}_i (T_i - T_i'), \ \forall \ i \in N_T \tag{3.10}$$

where T_i and T_i' are the temperatures of the supply and return circuits corresponding to node i. The mass flow rate balance at each node can be expressed as

$$\sum_{j:j\to i} \dot{m}_j^p - \sum_{k:i\to k} \dot{m}_k^p = \dot{m}_i, \forall \ i,j,k \in N_T \tag{3.11}$$

Equation (3.11) represents the flow continuity equation. The difference between the sum of flow rates entering a node and leaving a node equals the net consumption at that node. The column vectors of load, $\dot{m}_q$, and pipe mass flow rates, $\dot{m}$, can be related using the network incidence matrix, A_T as

$$A_T \dot{m} = \dot{m}_q \tag{3.12}$$

Given the DHS configuration, we can obtain the incidence matrix, A_T. Using the CFVT method, the load mass flow rate is a known quantity, and the individual pipe flow rates can be easily obtained using (3.12). The heat power balance at each node is

$$\sum_{j:j\to i} c_p \dot{m}_j^p T_j^{p+} = \sum_{k:i\to k} c_p \dot{m}_k^p T_k^{p-} + c_p \dot{m}_i T_i, \forall\ i,j,k \in N_T \tag{3.13}$$

where c_p is the specific heat of water. The electric boiler heat power is being supplied by EPS and the variable power can be directly summed up accordingly in (3.13). For the buses connected with EB, the heat balance equation can be expressed as

$$\sum_{j:j\to i} c_p \dot{m}_j^p T_j^{p+} = \sum_{k:i\to k} c_p \dot{m}_k^p T_k^{p-} + c_p \dot{m}_i T_i - h_{ebi} \tag{3.14}$$

The temperature at each node is equal to the inflow temperature of all the pipes connected to that node which gives

$$T_i = T_k^{p-},\ k : i \to k, \forall\ i,k \in N_T \tag{3.15}$$

The temperature drop along a pipe can be expressed as

$$\begin{aligned} T_j^{p+} - T_a &= (T_j^{p-} - T_a) e^{-\frac{\lambda L}{c_p \dot{m}_j^p}} \\ T_j^{p+} &= (T_j^{p-} - T_a) e^{-\frac{\lambda L}{c_p \dot{m}_j^p}} + T_a, \forall\ j \in N_T \end{aligned} \tag{3.16}$$

where L is the length of the pipe and T_a is the ambient temperature. By solving (3.12)-(3.16), the nodal temperatures of the DHS can be obtained. Both systems are linked using the electrical boilers, where they act as a load to the electrical system and as a source to the thermal system.

At node j, the heat power generated by the electrical boiler, h_{eb_j} and the electrical demand p_{eb_j} are related as follows:

$$h_{eb_j} = \eta \cdot p_{eb_j} \tag{3.17}$$

For a given s and $\dot{m}$, the complete set of solutions for the IEHS can be written as

$$\begin{aligned} \mathbb{X}(s, \dot{m}_q) : = \{x := (S, v, s_0, T) - x \text{ solves} \\ \text{(3.5-3.7),(3.9),(3.12)-(3.17) given } s, \dot{m}_q\} \end{aligned} \tag{3.18}$$

It should be noted that the presented DHS model represents a snapshot steady-state formulation and does not capture inter-temporal dynamics such as thermal storage evolution or pump scheduling over a 24-hour horizon. This completes the power flow modelling of both the electrical and heating systems. In the next section, a deterministic optimisation model to obtain the base case dispatch is presented. Next, to handle the uncertainties, a chance-constrained optimisation model, which can be solved using the scenario approach method, is explained. Later, the adopted scenario-based method and scenario reduction methodologies are discussed. The dynamic-dispatch coefficients to obtain the curtailments and electric boiler power levels are also discussed in this section.

3.3 Deterministic formulation

The objective of the proposed co-optimisation is to operate both the electrical and thermal systems efficiently and increase the utilisation of electrical boilers. In a renewable dominated system, the objective function aims to minimise the electrical losses and the conventional boiler power of DHS and maximise power transfer from the electrical system to the heating system, which in turn reduces curtailments.

Equation 3.19 represents a standard objective function formulation as proposed in [33]. The first term, $\sum r_{ij}|I_{ij}|^2$, corresponds to the minimisation of real power losses in the network.

The second term, $\sum c_i p_i^g$, represents the cost of real power generation, while the third term, $\sum \alpha_i |V_i|^2$, accounts for conservation voltage reduction (CVR) by promoting lower voltage magnitudes within allowable limits. The objective function takes the form

$$\min \sum r_{ij}|I_{ij}|^2 \; + \; \sum c_i p_i^g \; + \; \sum \alpha_i |V_i|^2 \tag{3.19}$$

for some given constants c_i, $\alpha_i \geq 0$.

The conic relaxation (3.9) is exact only if the objective is convex and strictly increasing [33]. Thus, each term in the summation (3.19) should be strictly increasing, which forces the constants c_i and α_i to be strictly $\geq$0. Also, the objective should be strictly increasing in I_{ij} and non-increasing in load. Thus, we cannot have a minimisation term for the curtailment power, p_{curt}. To avoid the p_{curt} term in the objective function, the electrical boiler power can take a negative coefficient as

$$f = \alpha_l \sum r_{ij} l_{ij} + \alpha_h \sum c_s h_s - \alpha_{eb} \sum p_{eb} \tag{3.20}$$

In the proposed method, voltage reduction is not considered in the objective; instead, they are taken care of using inequality constraints. The term $\sum r_{ij} l_{ij}$ represents electrical line losses, $\sum c_s h_s$ represents conventional heat generation, and $\sum p_{eb}$ represents electrical boiler power. As p_{eb} is a load term, it can take a negative coefficient, and is inline with the condition required for the relaxation to be exact. Here, c_s represents the per-unit operational cost associated with the conventional heat source h_s. Also, α_l, α_h, and α_{eb} are the weights associated with the electrical network losses, conventional heat power cost, and electric boiler powers, respectively. Weights can be tuned according to the operator's preference for the required objective.

All the electrical generation units will have upper and lower limits on the power generated.

Similarly, the conventional heating units of the DHS at bus i will have limits as

$$\begin{aligned} p_{gi_{min}} \leq p_{gi} \leq p_{gi_{max}} \\ h_{si_{min}} \leq h_{si} \leq h_{si_{max}} \end{aligned} \tag{3.21}$$

Also, the operational limits on the voltages, line currents, and bus temperatures at bus i can be considered as

$$\begin{aligned} v_{i_{min}} \leq v_i \leq v_{i_{max}}, \forall i \in N_E \\ l_{ij_{min}} \leq l_{ij} \leq l_{ij_{max}}, \forall (i,j) \in B_E \\ T_{i_{min}} \leq T_i \leq T_{i_{max}}, \forall i \in N_T \end{aligned} \tag{3.22}$$

Here, it is safe to assume f is convex. Also, f is strictly increasing in $l_{ij}, (i,j) \in B_E$, and independent of all S. Let,

$$\mathbb{S} := \{(S, v, s_0, s, T) | (v, s_0, s, T) \text{ satisfies } (3.21) - (3.22)\} \tag{3.23}$$

The complete deterministic optimal power flow problem of IEHS can be written as

$$\begin{aligned} \min_{x,s} \quad & f(l, h_s, p_{eb}) \\ \text{subject to} \quad & x \in \mathbb{X}, \quad (S, v, s_0, s, T) \in \mathbb{S} \end{aligned} \tag{3.24}$$

Here, $\hat{x}$ denotes optimal solution for the complete co-optimisation problem.

3.4 Chance-constrained co-optimisation formulation

The general chance-constrained optimisation problem contains probabilistic security constraints and aims to minimise the mean value of the objective function. The problem can be formulated

as

$$\begin{aligned} \min \quad & E(f) \\ \text{subject to} \quad & x \in \mathbb{X}, \quad (S, v, s_0, s, T) \in \mathbb{S} \\ & P(T_{i_{min}} \leq T_i \leq T_{i_{max}}) \geq 1 - \epsilon, \forall i \in N_T \\ & P(V_{i_{min}} \leq V_i \leq V_{i_{max}}) \geq 1 - \epsilon, \forall i \in N_E \\ & P(l_{ij_{min}} \leq l_{ij} \leq l_{ij_{max}}) \geq 1 - \epsilon, \forall (i,j) \in B_E \end{aligned} \tag{3.25}$$

Here $s, \dot{m}_q$ will also include the uncertainties, and the probabilistic constraints are complex to compute. The chance-constrained optimisation helps in solving this optimisation problem with uncertainties and a scenario-based approach is adopted here to solve the chance-constrained optimisation. The scenario approach of solving a chance-constrained framework works well with any probability distribution and also when the underlying probability distribution is not known but the samples are available from measurements which is the case in most practical situations [58].

The uncertainties in the system enforce that operational constraints are satisfied only up to a desired probability level $(1 - \epsilon)$. The parameter ϵ represents the acceptable risk of constraint violation, while the confidence level $(1 - \gamma)$ defines the statistical guarantee with which the scenario-based approximation satisfies the original chance constraints. Equivalently, γ denotes the probability that the scenario-based guarantee fails. A solution is said to be ϵ-level robustly feasible if, with confidence at least $(1 - \gamma)$, all operational constraints are violated in no more than an ϵ fraction of realisations. This interpretation directly links confidence to operational feasibility, ensuring that voltages, squared line currents, and temperatures remain within limits under uncertainty with high probability. For the solution of (3.28) to be valid, it has to be satisfied for a minimum number of scenarios, which are given by (3.26). For a given problem with n continuous variables and a γ confidence level, the number of scenarios is given as

$$\sum_{i=0}^{n-1} \binom{N}{i} \epsilon^i (1 - \epsilon)^{N-i} \leq \gamma \tag{3.26}$$

where N is the number of scenarios required to satisfy the inequality (3.26). Let N_{min} be the minimum number of scenarios to satisfy (3.26). Then, Monte Carlo simulations can be performed to generate N_{min} random scenarios and the set of scenarios is defined as O. Here, lower levels of γ imply stronger guarantees on feasibility at the cost of increased computational effort due to a larger required scenario set. The expected value of the objective function can be written as

$$E(f) = \sum_{k=1}^{N_{min}} \pi_k * \left\{ \alpha_l \sum_{(i,j)\in B_E} r_{ij} l_{ij} + \alpha_h \sum c_s h_s - \alpha_{eb} \sum p_{eb} \right\} \tag{3.27}$$

The complete chance-constrained optimisation problem can be written as

$$\begin{aligned} \min \quad & E(f) \\ \text{subject to} \quad & x_i \in \mathbb{X}_i, \quad (S, v, s_0, s, T)_i \in \mathbb{S}_i, \forall i \in O \end{aligned} \tag{3.28}$$

3.5 Dynamic dispatch of curtailments and electric boiler power

A linear rule is adopted here to dispatch the curtailments and electric boiler powers. The curtailment real power dispatch conforms with the standard characteristic curves as suggested in the German grid code [59]. Similarly, the electric boiler power is a real power demand on the EPS and thus a linear rule fits well for the dispatch.

For a RES connected at bus i, the linear dispatch rule for the curtailment is as follows,

$$p_{curt_i} = a_{i0} + \sum_{j\in B_R} a_{ij} p^f_{gj}, \forall i \in B_R \tag{3.29}$$

Similarly, for an electric boiler connected at bus i, the dispatch rule is as follows,

$$p_{EB_i} = b_{i0} + \sum_{j \in B_R} b_{ij} p_{gj}^f, i \in B_{EB} \tag{3.30}$$

Here a_{ij} and b_{ij} are linear variables and are obtained from the solutions of the chance-constrained optimisation framework set up in (3.28). The curtailed and EB powers for a particular scenario can be obtained using (3.5) and (3.17) respectively. In compact form, these two equations can be written as follows:

$$\begin{aligned} [p_{curt}] &= A \cdot [p_{RES}] \\ [p_{EB}] &= B \cdot [p_{RES}] \end{aligned} \tag{3.31}$$

Where A and B are the dynamic dispatch matrices for curtailments and EB power, respectively.

3.6 Scenario reduction methodology

Monte Carlo simulations are performed to generate different scenarios for load and RES generation. Here, the chance-constrained method is solved using a scenario-based approach. The bus voltages and temperatures are held within their operational limits with a given probability and confidence level. In the proposed method, electric boiler power and curtailment of RES are dynamically dispatched to reduce operational costs and network losses. The proposed method provides dynamic dispatch coefficients that can be used to obtain an exact dispatch after the uncertain parameters are revealed.

In the case of larger electrical grids, N_{min} is too large a number, and thus, the computational times of (3.25) will be practically infeasible. Scenario reduction methods have been useful in solving power management problems, and the same can be adopted here. A few of the popular methods are forward selection and backward reduction [60, 61]. Fast-forward reduction is the most popular and efficient method. However, these methods do not demonstrate scalability. A

SSR method proposed in [62] is proven to be efficient in handling larger datasets. Also, [63] proves that if the submodular function is monotone non-decreasing, then a solution within a constant factor of the optimum is guaranteed by a greedy algorithm. The scenario reduction technique solved using the greedy algorithm is proven to be a faster method [62] that beats the benchmark Fast Forward Selection (FFS) method to a greater extent, at least at the scale of 20 times faster for larger data sets of 10,000 scenarios. Thus, an accelerated greedy algorithm is adopted here to solve the submodular optimisation function and achieve faster computational times.

In this method, a similarity matrix for each scenario is needed to be calculated. Let s_i and s_j denote the set of uncertainties for scenario i and j respectively. Then, the similarity value, w_{ij} for each scenario is calculated using a radial basis kernel function (RBF) and l_2 norm as shown in (3.32)

$$w_{ij} = e^{-\frac{d_{ij}}{\lambda}} = e^{-\frac{||s_i - s_j||_2}{\lambda}} \tag{3.32}$$

where λ is the scaling factor for the distance measured in the exponent. The parameter λ controls the sensitivity of the similarity measure to the distance, $||s_i - s_j||_2$. In traditional RBF, $1/\lambda$ is the decay rate of the similarity distance. Thus, large λ leads to slower decay, and smaller λ leads to higher decay. The choice of λ directly influences how scenarios are clustered based on their distances. Larger λ values will promote selecting scenario subsets that span a wider range of the uncertainty space. Smaller λ values result in retaining scenarios in high-probability spaces of the uncertainty space and overlook less frequent scenarios. In the literature [64, 65], various tuning methods like empirical-based, performance-based, and objective-driven are discussed. A practical empirical method is to set λ to a fraction of $\max(||s_i - s_j||_2)$. Then, λ can be increased to select broader scenarios or can be reduced to select tighter clusters in higher probability regions.

Next, a cardinality-constrained maximisation is formulated as a facility location problem as

follows:

$$\begin{aligned} \max_{R} \quad & f_1(R) = \max_{R} \left(\sum_{i \in O} \max_{j \in R} w_{ij} \right) \\ \text{s.t.} \quad & \text{card}(R) \leq K \end{aligned} \tag{3.33}$$

Where O and R represent the original and reduced set of scenarios. K is the maximum size of the reduced set. The algorithm for solving this optimisation problem is adopted from [62] and tailored for this application.

The complete procedure is as follows:

1. **Generate initial scenario set:** Use Monte Carlo simulations to produce a large set of scenarios for uncertain parameters (e.g., RES generation, load demand). Denote the original set of scenarios as O, with cardinality N_{min}.

2. **Compute scenario similarity matrix:** For every pair of scenarios s_i and s_j, compute their similarity using a radial basis function (RBF) kernel with the l_2-norm distance as (3.32)

3. **Formulate the objective function:** The problem is framed as a cardinality-constrained maximisation as (3.33)

4. **Accelerated greedy selection:**

   (a) Initialise the reduced set $R \leftarrow \emptyset$.

   (b) At each iteration, select the scenario from $O \setminus R$ that yields the largest marginal increase in $f_1(R)$.

   (c) Use a priority queue to avoid recomputing gains for all scenarios, improving computational efficiency.

   (d) Repeat until $|R| = K$ or marginal improvement is below a threshold.

5. **Ranking and cut-off determination:** The greedy process produces a ranking of scenarios by importance. If K is not known in advance, the incremental improvements can be examined to determine a saturation point where additional scenarios yield negligible benefit.

6. **Assign probabilities:** Once R is chosen, redistribute probabilities using established rules so that the reduced set remains a valid probabilistic representation of the original uncertainty space.

7. **Integration into chance-constrained optimisation:** The reduced scenario set R is then used in the current chance-constrained co-optimisation, significantly reducing computational effort while retaining representativeness of the uncertainty set.

This adopted SSR method offers significant advantages as the problem size scales up, particularly for large initial scenario sets, which are common in IEHS with renewables. This formulation offers provable approximation guarantees, ensuring near-optimal selection while dramatically reducing computation time. Also, the greedy selection process minimises redundant calculations, enabling the method to handle tens of thousands of scenarios efficiently. This often achieves speedups of an order of magnitude compared to benchmark methods like FFS without sacrificing selection quality. Moreover, SSR not only selects a representative subset for a fixed cardinality but can also rank scenarios by importance, facilitating adaptive determination of the optimal number of scenarios based on marginal gains. This scalability, efficiency, and flexibility make SSR particularly well-suited for real-time or large-scale chance-constrained co-optimisation problems, where computational tractability is critical.

3.7 Solution methodology for the co-optimisation of IEHS

The complete algorithm to solve the co-optimisation of electrical and thermal systems is presented in this section. The load and RES uncertainties are considered, and the chance-

constrained optimisation is performed.

3.7.1 Steps involved in the algorithm

Step 1: Load the line parameter data of both the electrical and DHS networks. Electric boilers connect both networks, thus the information about their location is crucial. Load the forecasted values of the active, reactive power, and flow rates at each bus, forming the initial scenario set. The reduced scenario set is initialised with the set of all the forecasted values.

Step 2: Solve the deterministic optimisation using (3.24). The dynamic coefficients of the curtailment levels of each RES and electrical boiler power are obtained from this optimisation. These values are sufficient to obtain the operating voltage and temperature levels for different scenarios using the current injection (CI) method [66]. The CI method is a comparatively faster method to obtain the solutions of the network.

Step 3: At this step, for a given standard deviation level, Monte Carlo simulations are performed and a minimum number of scenarios as given by (3.26) are generated. Calculate the distance matrix using (3.32) and store it, as this can be used to run the SSR for multiple iterations in the algorithm. Using the dynamic coefficients from the deterministic solution, check the violations and prepare the failed scenarios set with all the current failed scenarios.

Step 4: Now, perform the SSR on the failed scenarios set and append them to the current reduced-scenario-set. Then perform the chance-constrained optimisation using (3.28) and obtain the dynamic dispatch coefficients of each RES and electric boiler.

Step 5: At this step, use the dynamic coefficients obtained from the previous step and verify if all the voltages and temperatures at each bus are respected for all the scenarios in the failed scenario set. If there are any further violations, update the failed scenario set with the current failed scenarios and go to step 4. Else, move to the next step.

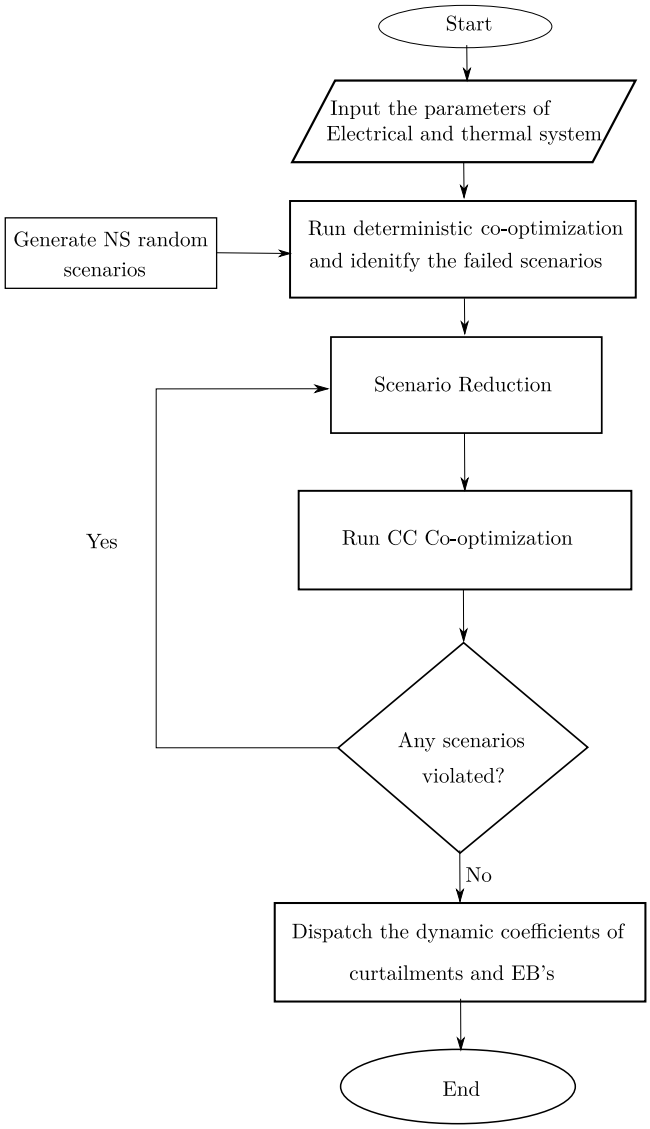


Figure 3.3: Flowchart for the chance-constrained optimisation

Step 6: At this step, all the coefficients obtained will ensure that the obtained solution is feasible for the chance-constrained framework with the pre-defined confidence level and can be dispatched.

The algorithm for the chance-constrained optimisation is summarised using a flowchart in Fig. 3.3.

3.7.2 Conclusions

This chapter introduced a comprehensive chance-constrained co-optimisation framework for IEHS, addressing the critical need to operate these systems reliably under growing uncertainty from RES and variable loads. The proposed method combines a deterministic base model with a probabilistic extension based on scenario analysis. This approach ensures that key operational limits, including voltage levels, line currents, and supply temperatures, are satisfied with high confidence under uncertainty.

Chapter 4

Numerical results

4.1 Introduction

This chapter presents the numerical evaluation of the chance-constrained co-optimisation framework for the IEHS model discussed which is discussed in Chapter 3. To validate the effectiveness of the presented models, simulations were conducted on two benchmark test systems, the IEEE 15-bus and the UKGDS 95-bus networks. Both systems are modified to incorporate RES and DHS, forming the integrated energy networks that reflect practical configurations. The performance of the model is assessed under both deterministic and stochastic (chance-constrained) scenarios, considering uncertainties in RES and load forecasts. These uncertainties are modelled as snapshot-based random variables at a given operating point, rather than as time-varying trajectories over a 24-hour horizon. Scenario samples are generated using Gaussian distributions around the forecasted values, with specified standard deviations to represent forecast errors.

The deterministic case serves as a baseline to highlight the advantages of the chance-constrained approach in terms of feasibility, operational security, and flexibility utilisation. Key performance metrics include the percentage of feasible scenarios, operational violations, dispatch behavior of electric boilers, and renewable curtailment levels under varying standard deviations. The results

demonstrate the scalability and robustness of the proposed model and illustrate how dynamic dispatch rules improve operational reliability across varying system sizes and uncertainty levels.

4.2 System model

The developed chance-constrained co-optimisation model is tested on a 3.5 GHz Intel Xeon E5 processor with 64 GB of RAM, where the proposed algorithm is programmed in Python and the optimisation problem is solved using the Gurobi 11.0 optimiser. The different test systems and specifications are as follows:

1. The first test system selected is an IEEE 15-bus distribution system [67] which is shown in Fig 4.1. The network configuration is modified to incorporate the RES and DHS networks at two of the buses. Each RES of 2 p.u. is connected at Bus 4 and 11 as shown in Fig. 4.1. Similarly, electric boilers are present on buses 12 and 14 which connect to the DHS networks. The configuration of each DHS is as shown in Fig. 4.2. The source $S1$ shown in Fig. 4.2 represents a conventional heat source. The load and RES profiles are assumed to be constant within each scenario and represent snapshot operating conditions. However, across scenarios, their values vary according to the adopted stochastic sampling process to capture forecast uncertainty. The network parameters are adopted from [37] and can be found in Appendix A. The rated voltage of the 15-bus network is 11 kV and the base power rating is 1 MVA.

2. The second test system considered is a 95-bus UKGDS system which is shown in Fig 4.3. Two renewable energy sources are connected to buses 40 and 90. Also, Electric boilers are present on buses 41 and 91 which connect to the DHS network. The rated voltage of the 95-bus network is 11 kV and the base power rating is 10 MVA. The network configuration and parameters can be found in [68]. The upper and lower limits on the voltages at each bus are 1.05 and 0.95 p.u. Similarly, the temperature limits in the DHS considered are

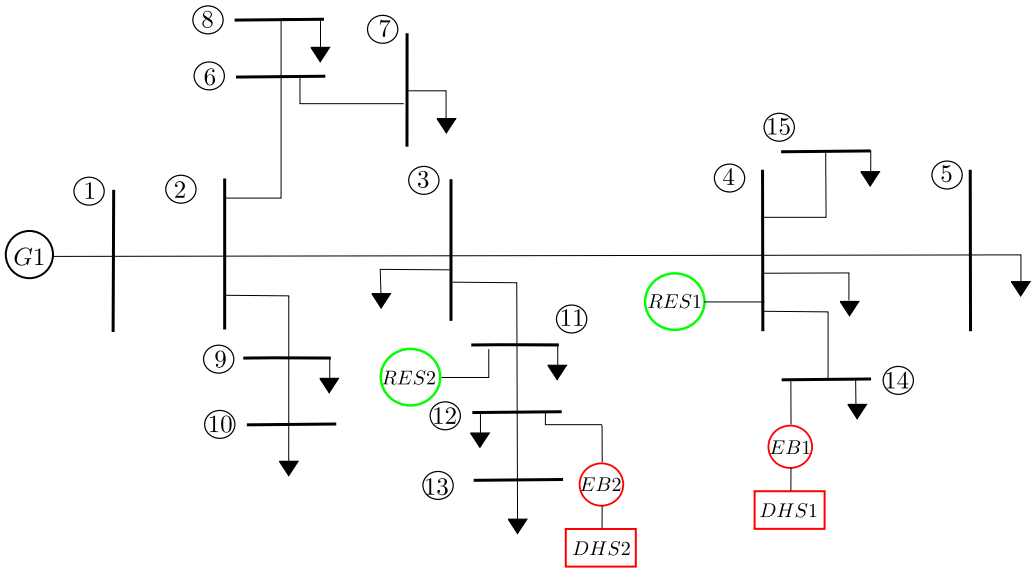


Figure 4.1: IEEE 15 bus test system [67]

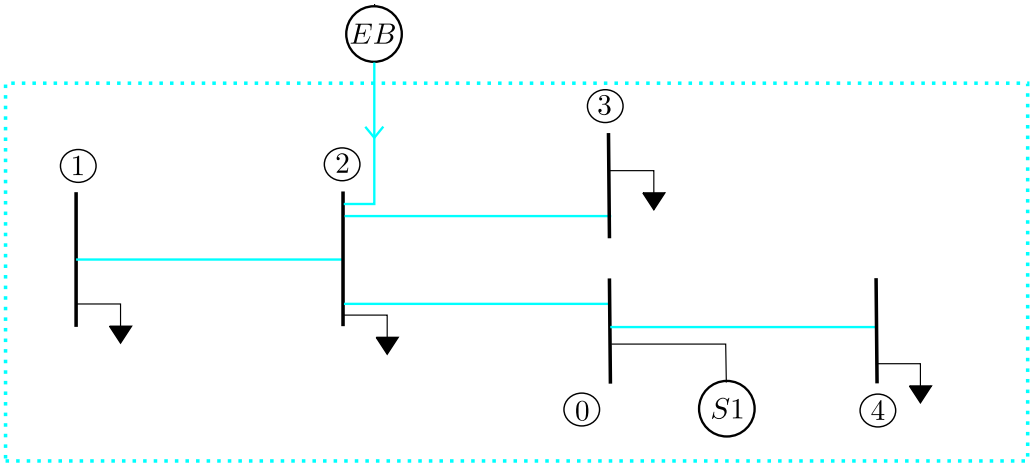


Figure 4.2: A 5-bus district heating test system

90 ^{o}C and 110 ^{o}C.

4.3 Solution using deterministic approach

15-bus test system

In the deterministic case, the optimisation is performed using the forecasted values of all the loads and active power of RES. The dispatch obtained is as follows, $P_{curt_3} = 1.133$ p.u., $P_{curt_{10}}$

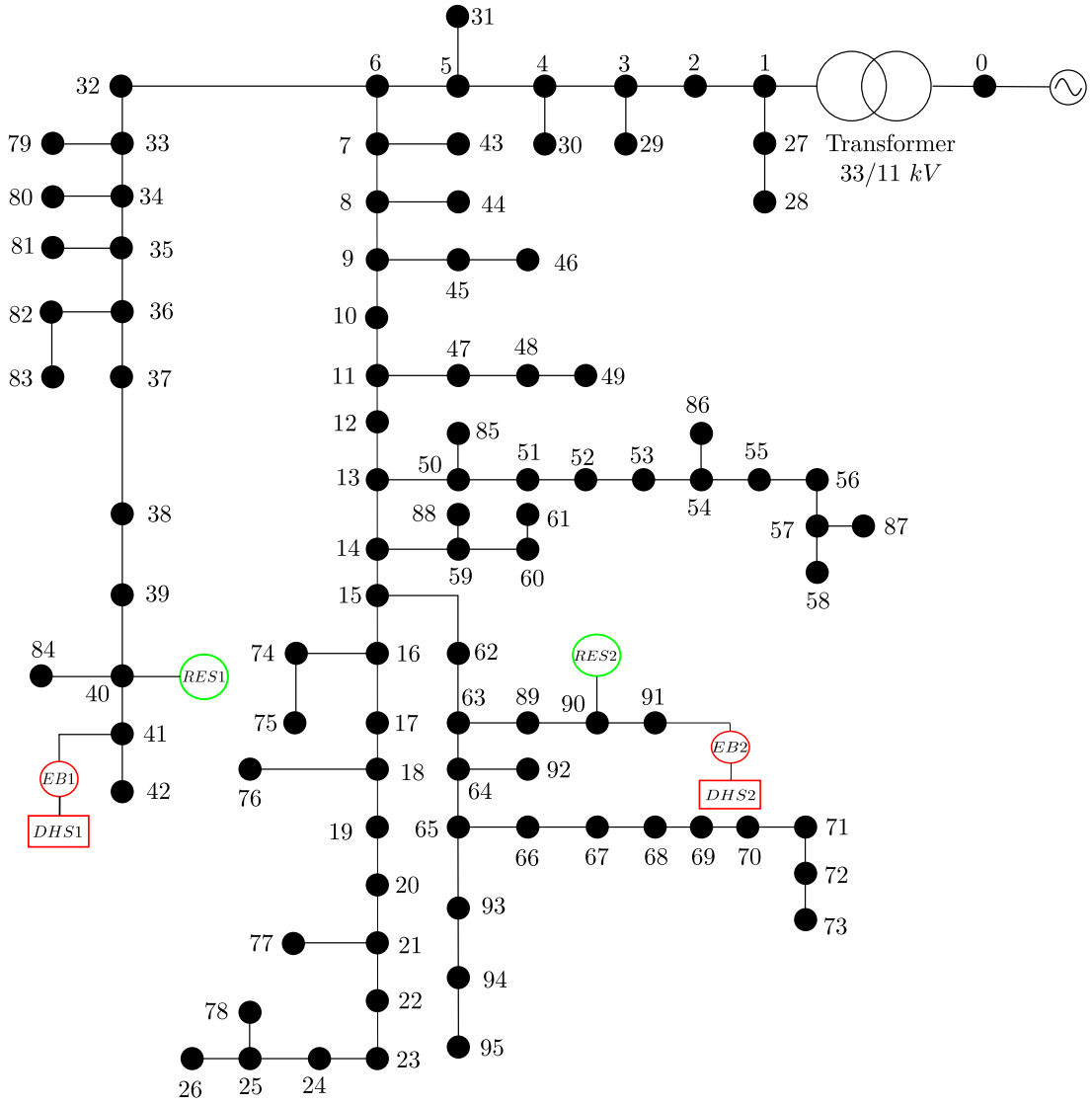


Figure 4.3: UKGDS 95-bus test system [68]

= 1.379 p.u. $P_{EB_{13}} = 0.394$ p.u. , $P_{EB_{11}} = 0.394$ p.u. Using this dispatch, posterior checks are performed on a dataset of 50,000 scenarios with a standard deviation (SD) of 0.05 for all the loads and RES. Around 31% of the scenarios are passed and 69% of the scenarios have severe violations. The voltage violations on bus 11, 12, 13, and 14, and temperature violations on DHS1 bus 1, 3, and 4 are as shown in Fig. 4.4. Four posterior data sets with different SDs of the RES forecast are generated. The percentage of scenarios passed for different standard deviations with the posterior set is as shown in Table 4.1. Among all these cases, only 25-30% of the scenarios are passed, and the majority of the scenarios fail.

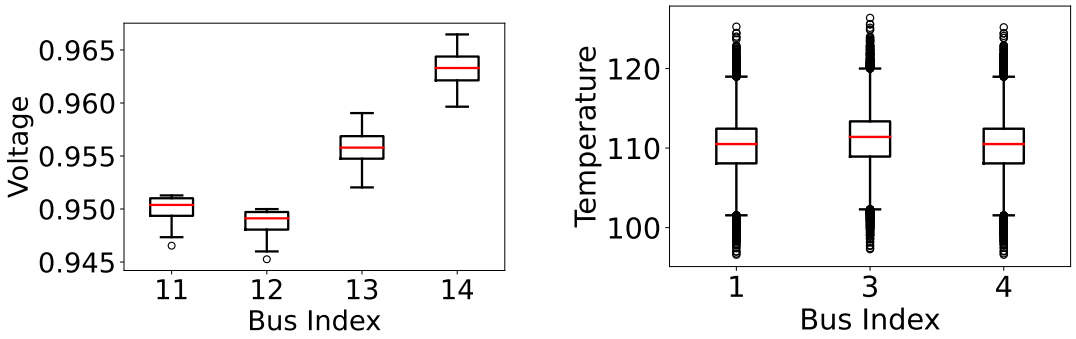


Figure 4.4: Voltage and temperature violations for the 15-bus system with deterministic dispatch

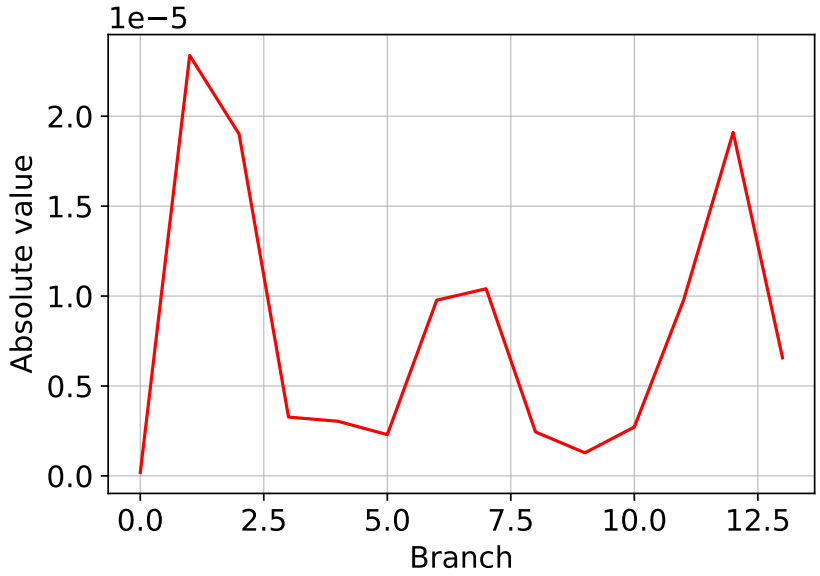


Figure 4.5: Relaxation gap of the inequality constraint of each branch for IEEE 15-bus deterministic case

95-bus test system

The deterministic dispatch obtained is as follows, $P_{curt_{40}} = 0.998$ p.u., $P_{curt_{90}} = 1.07$ p.u., $P_{EB_{41}} = 0.658$ p.u. , $P_{EB_{91}} = 0.658$ p.u. For the standard deviation of 0.05 on the loads and RES forecast, around 69.2% of the scenarios are passed and 30.8% of the scenarios have severe violations. The voltage violations on buses 39, 40, 41, 42, 89, 90, and 91 and the temperature violations on DHS1 bus 1, 3, and 4 are as shown in Fig. 4.6. The percentage of scenarios passed for different standard deviations with the posterior set is given in Table 4.1.

Table 4.1: Percentage of scenarios passed using deterministic approach for 15-bus test system

Standard deviation (SD)	**0.05**	**0.1**	**0.15**	**0.2**
Scenarios passed (%) for 15-bus system	31	29.9	26.7	24.5
Scenarios passed (%) for 95-bus system	30.8	31.1	30.9	30.7

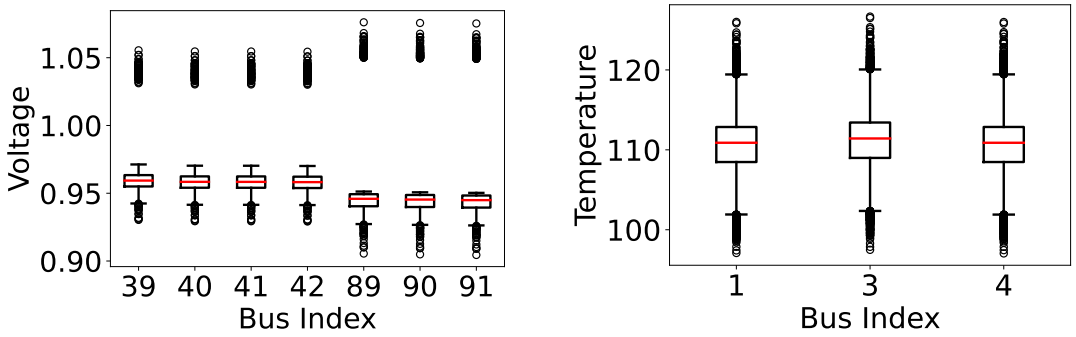


Figure 4.6: Voltage and temperature violations for the 95-bus system with deterministic dispatch

4.3.1 Discussion on relaxation gap

The equality condition in (3.8) is relaxed to an inequality to obtain (3.9). The relaxation is exact when a convex objective function is considered, and each term in the objective function is strictly increasing. The proposed formulation allows to obtain an exact solution which can be confirmed by verifying the relaxation gap. For IEEE 15-bus, it consists of 15 branches and thus there will be 15 inequalities to be relaxed. The absolute value of relaxation is plotted in Fig. 4.7. Here, the maximum relaxation gap is around 2.6e-5, which is negligible. Similarly, for UKGDS 95-bus system, a maximum relaxation gap of 1.5e-5 is observed as shown in Fig. 4.7. Thus, the obtained solutions are exact, and it is sufficient to optimise the relaxed model.

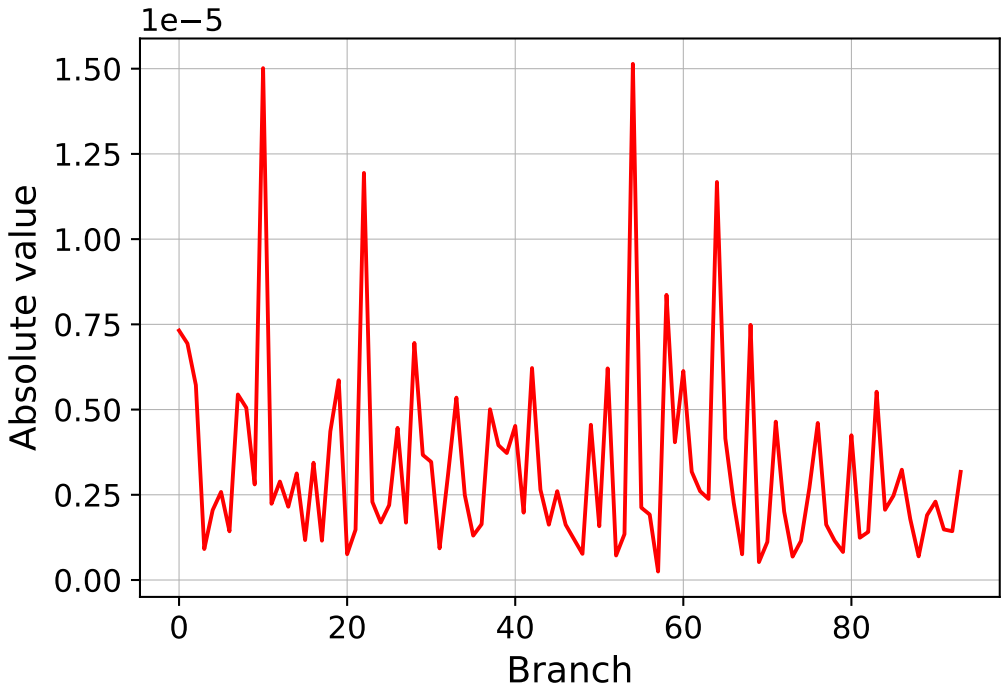


Figure 4.7: Relaxation gap of the inequality constraint of each branch for UKGDS 95-bus deterministic case

4.3.2 Solution using chance-constrained approach

15-bus test system

From (3.26), the minimum number of scenarios required to maintain the confidence level of γ=1e^{-10} is calculated as 3278 scenarios for a robustness parameter of $\epsilon = 0.02$. Using the deterministic dispatch as the starting solution, the violated scenarios are identified using the CI method. The proposed algorithm, as discussed in Section 3.7 is performed in iterations until all the 3278 scenarios become feasible. At each iteration, the solution is improved using (3.28), which is chance-constrained optimisation.

The expected values of EB power and curtailments for different SD values are shown in Fig. 4.8. It can be observed that the net expected utilisation of electric boilers is reduced in all the chance-constrained cases compared to the deterministic case. Similarly, the net expected curtailments are increased except for the 0.2 standard deviation case. However, the expected value of

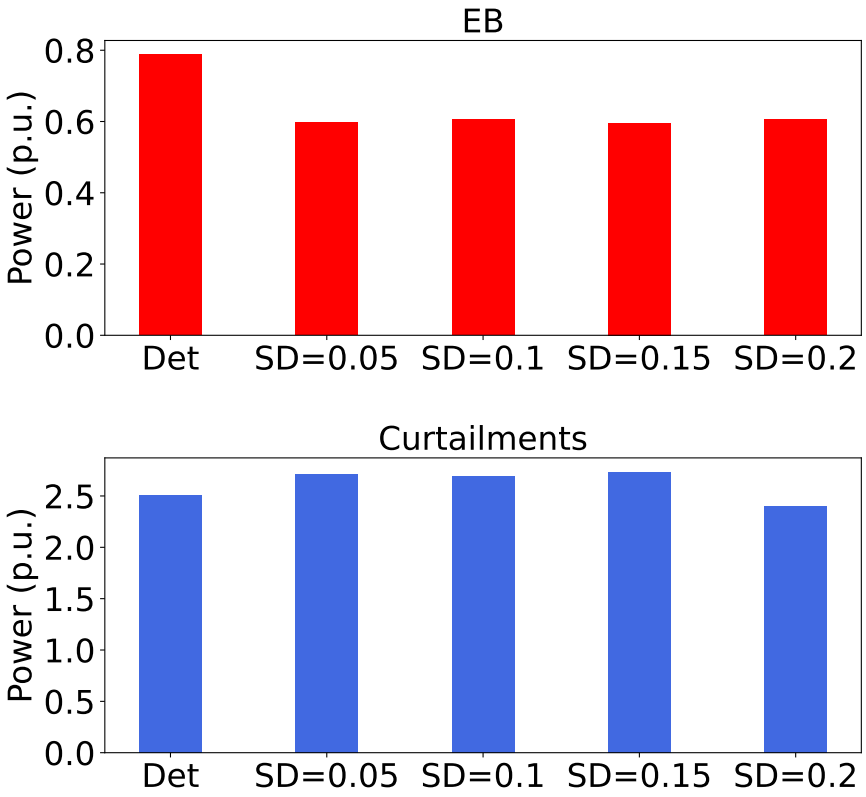


Figure 4.8: Comparison of expected values of 15-bus (a) electric boiler power (b)curtailments

the electrical network losses is lower in the case of the chance-constrained case compared to the deterministic case. This is a compromise on the reduction of EB power and increased curtailments for the reduction of operational violations. These expected values are computed over scenario samples generated from Gaussian distributions of load and RES forecast errors for each standard deviation level. The number of scenarios passed in the chance-constrained optimisation case is more when compared with the deterministic case and they are within the 2% failure range, which is expected given that ϵ is set at 0.02.

The total number of iterations, computational time, and reduced scenarios utilised to solve the cc-optimisation is shown in Table 4.3. For an SD of 0.2, the number of temperature and voltage failures at each iteration are shown in Fig. 4.9. The voltage and temperature violations for both deterministic and chance-constrained cases on the posterior data set are shown in Fig. 4.10. It can be observed that the number of violated scenarios and the magnitude of violation are significantly brought down in the chance-constrained case. Now, the dispatch parameters 'A'

Table 4.2: Summary of scenarios passed and violations for 15-bus test system

Standard deviation (SD)	**0.05**	**0.1**	**0.15**	**0.2**
Scenarios passed (DET)(%)	31%	29.9%	26.7%	24.5%
Scenarios passed (CC)(%)	98.96%	99.11%	98.51%	99.1%
Voltage violations	0	0	1	36
Temperature violations	517	445	744	414

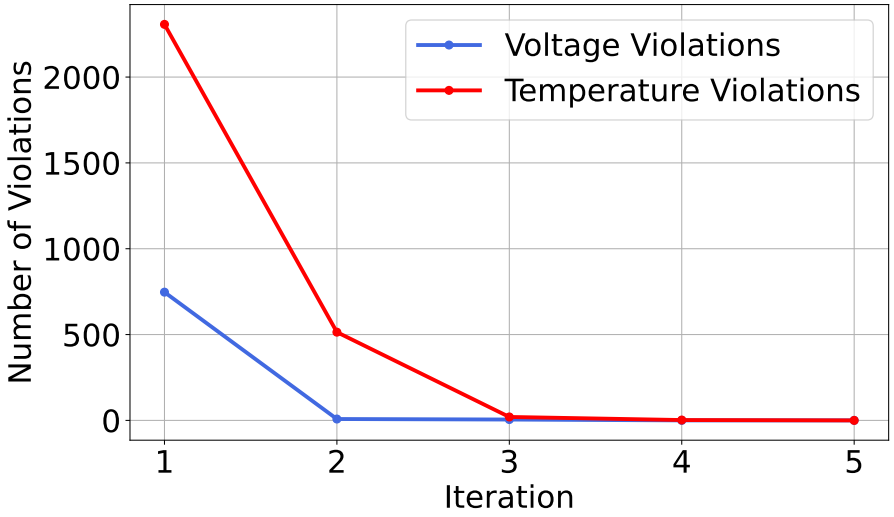


Figure 4.9: Voltage and temperature violations at each iteration for the 15-bus system with SD=0.2

and 'B' can be written as follows,

$$A = \begin{bmatrix} a_{10} & a_{11} & a_{12} \\ a_{20} & a_{21} & a_{22} \end{bmatrix}, \qquad B = \begin{bmatrix} b_{10} & b_{11} & b_{12} \\ b_{20} & b_{21} & b_{22} \end{bmatrix},$$

$$p_{RES} = \begin{bmatrix} 1 & p_3 & p_{10} \end{bmatrix}^T.$$

The matrix p_{RES} is dependent on the real power forecast at bus 3 and 10. The dispatch parameters for different cases of SD are as shown in Table 4.4. It can be observed that the curtailment levels of a renewable source connected at bus i are strongly dependent on the parameter a_{ii} which shows that the amount of power to be curtailed is dependent on the power forecast at that bus. Whereas the power dispatch of the electric boiler connected at bus i has

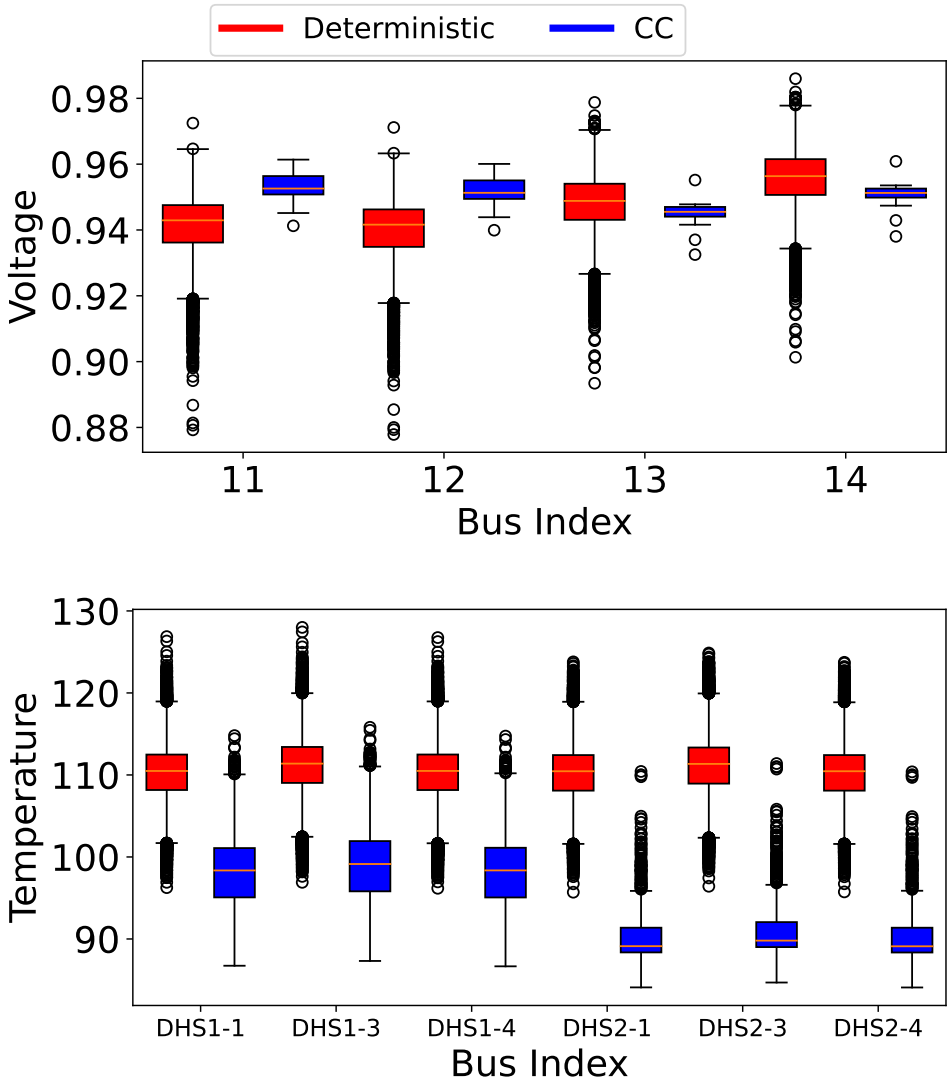


Figure 4.10: Comparison of violations in the posterior set for 15-bus DET and CC cases (a) voltage violations (b) temperature violations

a significant parameter b_{i0} and the other parameters are less significant.

To assess the impact of spatial placement of the DHS relative to RES, multiple location-based cases are considered. In each case, the RES units are connected to the same set of buses, while the electric boilers (and hence the associated DHS networks) are connected to different buses in the electrical network. These locations are deliberately selected to represent both electrically closer and farther configurations with respect to the RES buses, allowing the influence of network topology on curtailment, EB utilisation, and losses to be examined. The specific RES and EB bus locations corresponding to each case are summarised in Table 4.5.

Table 4.3: Number of iterations and reduced scenarios for 15-bus system

SD	**0.05**	**0.1**	**0.15**	**0.2**
No. of reduced scenarios	56	64	60	63
No. of Iterations	4	5	6	5
Simulation time (s)	122.2	128.54	130.265	130.9

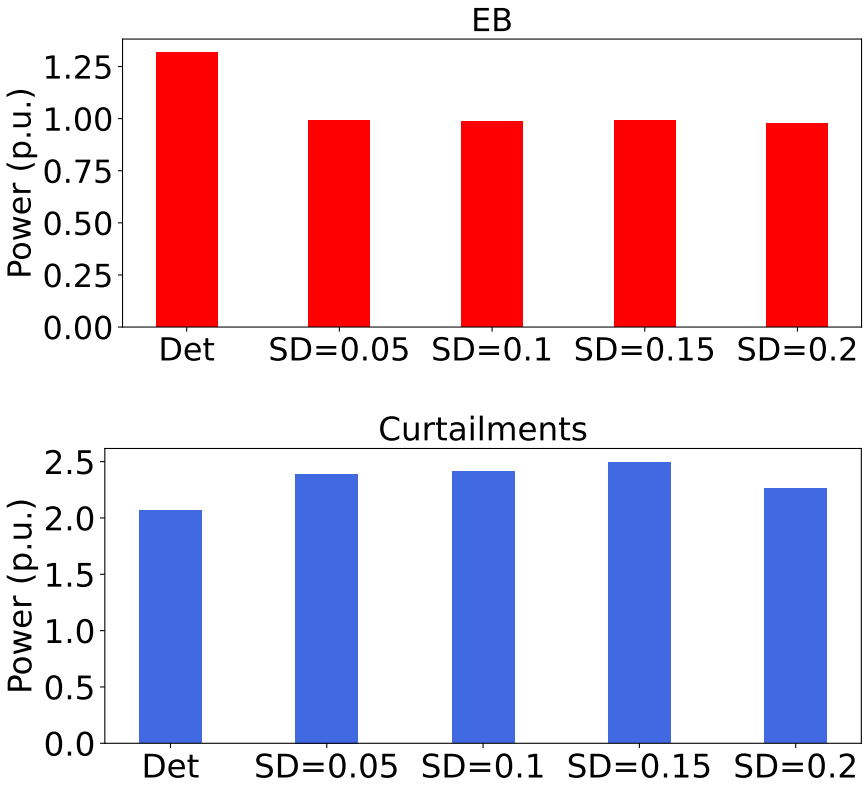


Figure 4.11: Comparison of expected values of 95-bus (a) electric boiler power (b) curtailments

95-bus test system

From (3.26), the minimum number of scenarios required to maintain the confidence level of γ=1e-10 is calculated as 8826 for a robustness parameter of ϵ=0.02. The expected values of EB power and curtailments for different SD values are shown in Fig. 4.11.

It can be observed that the net expected utilisation of electric boilers is reduced in all the chance-constrained cases compared to the deterministic case. Similarly, the net expected curtailments are increased in all the cases. The number of scenarios passed in the CC-optimisation case is

Table 4.4: Coefficients of the dynamic dispatch variables of the 15-bus test system for different SDs

	SD=0.05	SD=0.1	SD=0.15	SD=0.2
a_{10}	0	0	0	0
a_{11}	0.74	0.72	0.749	0.633
a_{12}	0	0.015	0	0
a_{20}	0	0	0	0
a_{21}	0	0	0	0.315
a_{22}	0.617	0.61	0.618	0.242
b_{10}	0.2655	0.245	0.242	0.3
b_{11}	0	0	0	0
b_{12}	0.17	0.033	0.026	0.005
b_{20}	0.26	0.2964	0.221	0.296
b_{21}	0.019	0	0.006	0
b_{22}	0	0	0.036	0

more when compared with the deterministic case and it is within the 2% failure range for a posterior set of 50,000 scenarios. Now, for the dispatch, we can write the p_{RES} matrix in terms of real power forecast at bus 40 and 90 as, $p_{RES} = \begin{bmatrix} 1 & p_{40} & p_{90} \end{bmatrix}^T$.

The dispatch parameters for different cases of SD's are shown in Table 4.7. The total number of iterations, computational time, and reduced scenarios utilised to solve the cc-optimisation is shown in Table 4.8. A similar trend for the IEEE 15 bus can be observed here too. The curtailment level of the renewable source connected at bus i is strongly dependent on the parameter a_{ii}. The dispatch of the electric boiler power connected at bus i is strongly dependent on b_{i0}. Now, the DHS is connected to different buses and the dispatch parameters for SD=0.05 are shown in Table 4.9. In this case, the dependence on b_{21} for the electric boiler power dispatch can also be observed.

Table 4.5: Dynamic dispatch coefficients of the 15-bus test system for different locations of DHS network

	Case 1	**Case 2**	**Case 3**	Case 4
RES Bus no.	{3,10}	{3,10}	{3,10}	{3,10}
EB Bus no.	{13,11}	{7,2}	{6,9}	{14,4}
a_{10}	0	0	0	0
a_{11}	**0.74**	**0.832**	**0.788**	**0.769**
a_{12}	0	0	0.06	0.12
a_{20}	0	0	0	0
a_{21}	0	0	0	0
a_{22}	**0.617**	**0.638**	**0.674**	**0.469**
b_{10}	**0.2655**	**0.2657**	**0.266**	**0.09**
b_{11}	0	0	0	0.065
b_{12}	0.17	0.0169	0.169	0.036
b_{20}	**0.26**	**0.26**	**0.065**	**0.26**
b_{21}	0.019	0.019	0.11	0.019
b_{22}	0	0	0	0

4.4 Conclusions

The numerical results validate the efficacy of the proposed chance-constrained co-optimisation framework in enhancing the operational reliability and flexibility of IEHS. Compared to deterministic dispatch, the chance-constrained approach significantly reduces voltage and temperature violations while ensuring a high percentage of feasible scenarios within predefined risk limits. For both the 15-bus and 95-bus test systems, the model effectively adapts to increasing uncertainty through dynamic dispatch rules that adjust electric boiler usage and RES curtailment based on forecast deviations. Moreover, the study confirms that the relaxation of non-convex constraints introduces negligible error, ensuring the practical applicability of the convexified formulation. The framework also exhibits adaptability to varying DHS con-

Table 4.6: Summary of scenarios passed and violations for 95-bus test system

Standard deviation (SD)	**0.05**	**0.1**	**0.15**	**0.2**
Scenarios passed (DET)(%)	30.8%	31.1%	30.9%	30.7%
Scenarios passed (CC)(%)	98.8%	98.6%	98.4%	98.3%
Voltage violations	0	0	0	0
Temperature violations	588	673	798	813

figurations and RES placements, making it suitable for real-world deployment in flexible and uncertain multi-energy environments. These findings affirm the potential of chance-constrained methods to support secure, cost-effective, and resilient multi-energy system operations.

Table 4.7: Coefficients of the dynamic dispatch variables of the 95-bus test system for different SD's

	SD=0.05	SD=0.1	SD=0.15	SD=0.2
a_{10}	0	0	0	0
a_{11}	0.62	0.632	0.547	0.562
a_{12}	0	0	0.078	0
a_{20}	0	0	0	0
a_{21}	0	0	0	0.146
a_{22}	0.558	0.552	0.612	0.39
b_{10}	0.511	0.5	0.332	0.48
b_{10}	0	0	0.045	0
b_{12}	0	0	0.042	0
b_{20}	0.09	0.477	0.399	0.48
b_{21}	0.11	0	0.032	0
b_{22}	0.08	0	0	0.0122

Table 4.8: Number of iterations and reduced scenarios for 95-bus system

SD	**0.05**	**0.1**	**0.15**	**0.2**
No. of reduced scenarios	60	60	55	60
No. of Iterations	5	5	4	5
Simulation time (s)	977.6	1012.4	976.7	1085.36

Table 4.9: Dynamic dispatch coefficients of the 95-bus test system for different locations of DHS network

	Case 1	**Case 2**	**Case 3**
RES Bus no.	{40,90}	{40,90}	{40,90}
EB Bus no.	{41,91}	{12,74}	{33,11}
a_{10}	0	0	0
a_{11}	**0.62**	**0.777**	**0.834**
a_{12}	0	0	0.027
a_{20}	0	0	0
a_{21}	0	0	0
a_{22}	**0.558**	**0.573**	**0.59**
b_{10}	**0.511**	**0.511**	**0.511**
b_{11}	0	0	0
b_{12}	0	0	0
b_{20}	**0.09**	**0.09**	**0.095**
b_{21}	0.11	0.115	0.115
b_{22}	0.08	0.077	0.076

Chapter 5

Conclusions and future work

This chapter summarises the key findings of the research and discusses potential directions for future work. The thesis aimed to focus on the co-optimisation frameworks for scheduling of IEHS, mainly with the objective of minimising operational costs and renewable energy curtailment. Using a test system inspired by the Bornholm Island energy infrastructure, the research investigated the coordinated operation of conventional and renewable generators, flexible electrical and thermal loads, and storage units. In addition to the deterministic linear model, a chance-constrained co-optimisation framework was developed to address uncertainties in renewable generation and demand forecasts. A scenario-based approach was adopted to capture stochastic variations, and a scenario reduction technique was implemented to improve computational efficiency while maintaining solution quality. This chapter presents the conclusions drawn from all the chapters presented and outlines several possible extensions that could enhance the scope and originality of the current work.

5.1 Conclusions

This thesis mainly addressed the challenges of co-optimisation of IEHS. The key conclusions of this thesis are as follows:

1. This thesis has developed deterministic and chance-constrained co-optimisation frameworks for the coordinated day-ahead scheduling of integrated electrical and heating systems (IEHS). By explicitly modelling the operational coupling between electrical and thermal networks, the proposed formulations demonstrate that joint optimisation is essential to achieve cost-efficient and low-curtailment operation in systems with high renewable energy penetration. Numerical results consistently show that co-optimisation outperforms independent operation by exploiting cross-sector flexibility rather than relying on additional infrastructure.

2. The deterministic linear co-optimisation framework provides a practical and computationally efficient method for scheduling IEHS. Using a test system inspired by the Bornholm Island energy infrastructure, it is shown that flexible thermal loads, electric boilers, and thermal storage significantly enhance system-wide flexibility, leading to reductions in operating costs and renewable energy curtailment.

3. Recognising the limitations of deterministic scheduling under uncertainty, this thesis extends the co-optimisation problem to a chance-constrained formulation that explicitly accounts for stochastic variations in renewable generation and demand. The scenario-based approach allows probabilistic operational constraints to be enforced within predefined confidence levels, thereby improving system reliability while maintaining economic efficiency.

4. The computational burden associated with scenario-based chance-constrained optimisation is addressed through the application of scenario reduction techniques. Numerical studies demonstrate that the reduced scenario set preserves solution quality and reliabil-

ity guarantees while enabling the stochastic co-optimisation problem to be solved within practical computation times, making the approach suitable for real-world applications.

5. Dynamic dispatch rules are incorporated within the chance-constrained framework to enable real-time adjustment of renewable curtailment and electric boiler operation in response to forecast deviations. This additional recourse mechanism enhances operational resilience and reduces the conservativeness typically associated with stochastic optimisation, allowing the system to better adapt to real-time conditions.

6. The scalability and generality of the proposed frameworks are demonstrated by applying the chance-constrained co-optimisation model to larger benchmark systems, including the IEEE 15-bus and UKGDS 95-bus networks. The results confirm that the methodology is not restricted to small or islanded systems and can be extended to realistic distribution networks with diverse operating conditions.

7. Overall, the thesis establishes that co-optimisation of IEHS is a key enabler for the energy transition, allowing higher renewable penetration, reduced emissions, and improved operational robustness. The proposed modelling framework is general and extensible, providing a foundation for future integration of additional energy vectors such as gas, hydrogen, and cooling systems, and supporting the evolution toward fully sector-coupled energy systems.

5.2 Future work

While the current work provides a solid foundation for co-optimising IEHS, several important directions remain for future research. These extensions would not only improve the accuracy and originality of the current models but also support broader adoption and operational integration in real-world energy systems.

- **Uncertainty modelling:** Although this work introduces a chance-constrained approach

to handle forecast uncertainties, further exploration into advanced stochastic optimisation techniques such as distributionally robust optimisation, and adaptive scenario-based formulations can enhance decision-making under deep uncertainty. These methods can improve the system's responsiveness to high levels of variability in renewable energy sources and demand.

- **Multi-Time scale coordination:** Future work could address the coordination between day-ahead, intraday, and real-time operational layers. Such multi-timescale frameworks are essential for dealing with forecast errors, ramping needs, and dynamic load behaviors, especially in systems with high renewable penetration.

- **Sector coupling with additional energy vectors:** The integration of other energy carriers, such as natural gas, hydrogen, and district cooling, can extend the model into a full multi-energy system. Such coupling can enhance flexibility, support decarbonisation strategies, and facilitate the design of energy hubs or prosumer-oriented communities.

- **Decentralised or market-based operation:** The centralised optimisation approach used in this thesis could be extended to distributed or hierarchical control frameworks. Future research may explore agent-based models, peer-to-peer energy trading, and market-based mechanisms for demand-side flexibility in integrated energy communities.

- **Experimental validation and real-time testing:** To bridge the gap between theory and practice, the models developed here can be tested using hardware-in-the-loop simulations or applied to real-world testbeds, such as Bornholm Island. Such a validation would uncover practical challenges, including communication delays, control limitations, and data availability, which are critical for deployment readiness.

Overall, advancing these research directions will be essential for realising the next generation of smart, sustainable, and resilient energy systems. By extending the current modelling approaches, future studies can support more adaptive and robust decision-making frameworks that

align with evolving energy policy targets and the increasing complexity of integrated energy infrastructures.

Bibliography

[1] P. Mancarella, S. Mhanna, and E. A. M. Ceseña, "Multienergy system scheduling: Allocating resources and flexibility across energy vectors," *IEEE Power and Energy Magazine*, vol. 23, no. 3, pp. 65–77, 2025.

[2] Integrating solar and wind-global experience and emerging challenges. [Online]. Available: https://iea.blob.core.windows.net/assets/4e495603-7d8b-4f8b-8b60-896a5936a31d/IntegratingSolarandWind.pdf

[3] Britain wastes enough wind generation to power 1 million homes. [Online]. Available: https://carbontracker.org/britain-wastes-enough-wind-generation-to-power-1-million-homes/

[4] Renewables 2023 : Analysis and forecast to 2028. [Online]. Available: https://iea.blob.core.windows.net/assets/96d66a8b-d502-476b-ba94-54ffda84cf72/Renewables_2023.pdf

[5] D. Wang, L. Liu, H. Jia, W. Wang, Y. Zhi, Z. Meng, and B. Zhou, "Review of key problems related to integrated energy distribution systems," *CSEE Journal of Power and Energy Systems*, vol. 4, no. 2, pp. 130–145, 2018.

[6] "Heating," https://www.iea.org/fuels-and-technologies/heating, 2022, [Online; accessed 30-05-2023].

[7] S. Long, "Generalised modelling framework for multi-energy systems with model predictive control applications," Ph.D. dissertation, 2020.

[8] M. Geidl and G. Andersson, "Optimal power flow of multiple energy carriers," *IEEE Transactions on Power Systems*, vol. 22, no. 1, pp. 145–155, 2007.

[9] W. Kong, X. Wu, G. Geng, E. Li, X. Zhang, and W. Tangi, "Optimal scheduling of multi-energy system in rural farms for biomass/photovoltaic/geothermal efficient utilization," in *2021 IEEE Sustainable Power and Energy Conference (iSPEC)*, 2021, pp. 944–951.

[10] X. Gu and Z. Chen, "Multi-time-scale scheduling optimization of regional multi-energy systems considering source-load uncertainty," in *2021 13th International Conference on Measuring Technology and Mechatronics Automation (ICMTMA)*, 2021, pp. 198–201.

[11] Y. Sun, Y. Teng, and S. Yang, "Optimization model of multi-energy system based on multi-source energy storage," in *2021 13th International Conference on Measuring Technology and Mechatronics Automation (ICMTMA)*, 2021, pp. 216–219.

[12] Z. Yongjie, L. Yuping, H. Bing, Z. Wei, W. Runyi, C. Dong, and S. Yonghui, "Multi-objective optimization dispatch for regional integrated power and heat energy system considering adjustable heat load," in *2021 IEEE Sustainable Power and Energy Conference (iSPEC)*, 2021, pp. 810–815.

[13] J. Wei, J. Wang, H. Gao, and X. Gao, "Optimal operation of micro integrated energy systems considering electrical and heat load classification and scheduling," in *2017 IEEE Conference on Energy Internet and Energy System Integration (EI2)*, 2017, pp. 1–6.

[14] A. Krishnan, P. K. Ray, and A. K. Barisal, "Optimal scheduling of multi-energy systems with load scheduling in multiple energy streams," in *2022 IEEE International Conference on Power Electronics, Smart Grid, and Renewable Energy (PESGRE)*, 2022, pp. 1–7.

[15] S. Ahmad, M. Shafiullah, C. B. Ahmed, and M. Alowaifeer, "A review of microgrid energy management and control strategies," *IEEE Access*, vol. 11, pp. 21 729–21 757, 2023.

[16] F. Hu, F. Wang, R. Wu, S. Wu, K. Wang, C. Huang, Y. Chen, and Z. Li, "Review on modeling and optimal scheduling in integrated energy systems," in *2021 IEEE 5th Conference on Energy Internet and Energy System Integration (EI2)*, 2021, pp. 1698–1703.

[17] W. Zheng, H. Lu, M. Zhang, Q. Wu, Y. Hou, and J. Zhu, "Distributed energy management of multi-entity integrated electricity and heat systems: A review of architectures, optimization algorithms, and prospects," *IEEE Transactions on Smart Grid*, vol. 15, no. 2, pp. 1544–1561, 2024.

[18] R. Zhang, Y. Chen, B. Li, T. Jiang, X. Li, H. Chen, and R. Ning, "Adjustable robust interval economic dispatch of integrated electricity and district heating systems under wind power uncertainty," *Energy Reports*, vol. 8, pp. 13 138–13 149, 2022. [Online]. Available: https://www.sciencedirect.com/science/article/pii/S2352484722018108

[19] B. Deng, J. Fang, Q. Hui, T. Zhang, Z. Chen, Y. Teng, and X. Xi, "Optimal scheduling for combined district heating and power systems using subsidy strategies," *CSEE Journal of Power and Energy Systems*, vol. 5, no. 3, pp. 399–408, 2019.

[20] C. He, L. Wu, T. Liu, and M. Shahidehpour, "Robust co-optimization scheduling of electricity and natural gas systems via admm," *IEEE Transactions on Sustainable Energy*, vol. 8, no. 2, pp. 658–670, 2017.

[21] S. P. Polisetty, T. Joseph, A. Turk, E. I. Batzelis, B. C. Pal, G. Yang, and P. Kotsampopoulos, "Co-optimization of electrical and district heating networks: Bornholm case study," in *2023 62nd IEEE Conference on Decision and Control (CDC)*, 2023, pp. 2549–2554.

[22] T. Ding, H. Sun, F. Harley, F. Li, and R. Bo, "Bi-level linear programming based interval optimization for sced in the presence of wind power uncertainty," in *2014 IEEE PES General Meeting — Conference & Exposition*, 2014, pp. 1–5.

[23] H. Shuai, J. Fang, X. Ai, Y. Tang, J. Wen, and H. He, "Stochastic optimization of economic dispatch for microgrid based on approximate dynamic programming," *IEEE Transactions on Smart Grid*, vol. 10, no. 3, pp. 2440–2452, 2019.

[24] E. Du, N. Zhang, B.-M. Hodge, Q. Wang, Z. Lu, C. Kang, B. Kroposki, and Q. Xia, "Operation of a high renewable penetrated power system with csp plants: A look-ahead stochastic unit commitment model," *IEEE Transactions on Power Systems*, vol. 34, no. 1, pp. 140–151, 2019.

[25] H. Qiu, W. Gu, Y. Xu, and B. Zhao, "Multi-time-scale rolling optimal dispatch for ac/dc hybrid microgrids with day-ahead distributionally robust scheduling," *IEEE Transactions on Sustainable Energy*, vol. 10, no. 4, pp. 1653–1663, 2019.

[26] M. Xie, P. Cheng, and S. Ke, "Power system dynamic economic dispatch with wind-solar integration based on particle swarm intelligent searching algorithm," in *2017 China International Electrical and Energy Conference (CIEEC)*, 2017, pp. 252–257.

[27] N. Sensoy and G. Ceyhan, "A genetic algorithm to solve day-ahead energy market clearing problem under network constraints," in *2018 15th International Conference on the European Energy Market (EEM)*, 2018, pp. 1–6.

[28] M. Wang, H. Bai, M. Zhou, and J. Wang, "A generation-reserve co-optimization dispatching model for wind power integrated power system based on risk reserve constraints," in *International Conference on Renewable Power Generation (RPG 2015)*, 2015, pp. 1–6.

[29] M. A. Mirzaei, M. Nazari-Heris, B. Mohammadi-Ivatloo, K. Zare, M. Marzband, and A. Anvari-Moghaddam, "A novel hybrid framework for co-optimization of power and natural gas networks integrated with emerging technologies," *IEEE Systems Journal*, vol. 14, no. 3, pp. 3598–3608, 2020.

[30] C. He, L. Wu, T. Liu, and M. Shahidehpour, "Robust co-optimization scheduling of electricity and natural gas systems via admm," *IEEE Transactions on Sustainable Energy*, vol. 8, no. 2, pp. 658–670, 2017.

[31] C. He, L. Wu, T. Liu, and Z. Bie, "Robust co-optimization planning of interdependent electricity and natural gas systems with a joint n-1 and probabilistic reliability criterion," *IEEE Transactions on Power Systems*, vol. 33, no. 2, pp. 2140–2154, 2018.

[32] E. A. Martínez Ceseña, E. Loukarakis, N. Good, and P. Mancarella, "Integrated electricity– heat–gas systems: Techno–economic modeling, optimization, and application to multienergy districts," *Proceedings of the IEEE*, vol. 108, no. 9, pp. 1392–1410, 2020.

[33] M. Farivar and S. H. Low, "Branch flow model: Relaxations and convexification—part i," *IEEE Transactions on Power Systems*, vol. 28, no. 3, pp. 2554–2564, 2013.

[34] R. Jabr, "Radial distribution load flow using conic programming," *IEEE Transactions on Power Systems*, vol. 21, no. 3, pp. 1458–1459, 2006.

[35] A. Babiker, S. S. Ahmad, I. Ahmed, M. Khalid, M. A. Abido, and F. Saleh Al-Ismail, "Optimal power flow: A review of state-of-the-art techniques and future perspectives," *IEEE Access*, vol. 13, pp. 60 012–60 039, 2025.

[36] D. J. Ahmad, N. Hariyanto, and U. Khayam, "Issues, challenges, and solution options for on-grid multi-microgrid game theory: A systematic review," *IEEE Access*, vol. 13, pp. 76 574–76 608, 2025.

[37] X. Liu, "Combined analysis of electricity and heat networks," Ph.D. dissertation, 2013.

[38] W. Zheng, Y. Hou, and Z. Li, "A dynamic equivalent model for district heating networks: Formulation, existence and application in distributed electricity-heat operation," *IEEE Transactions on Smart Grid*, vol. 12, no. 3, pp. 2685–2695, 2021.

[39] Z. Wang, N. Zhang, Y. Zhang, X. Lin, and F. Qin, "A study on hydraulic balance optimization of district heating system based on data-mechanism fused model," in *2021 IEEE 5th Conference on Energy Internet and Energy System Integration (EI2)*, 2021, pp. 4046–4050.

[40] A. Sorocins, J. Nagla, and V. Zentins, "District heating simulation model development to solve optimization problems in the market conditions," in *2020 IEEE 61th International Scientific Conference on Power and Electrical Engineering of Riga Technical University (RTUCON)*, 2020, pp. 1–5.

[41] W. Tang and S. Huang, "Load flow analysis of district heating systems by a newton-raphson method," in *2019 IEEE 3rd Conference on Energy Internet and Energy System Integration (EI2)*, 2019, pp. 1357–1362.

[42] K. Paridari, A. Parisio, H. Sandberg, and K. H. Johansson, "Robust scheduling of smart appliances in active apartments with user behavior uncertainty," *IEEE Transactions on Automation Science and Engineering*, vol. 13, no. 1, pp. 247–259, 2016.

[43] Y. Qiu, Q. Li, Y. Ai, W. Chen, M. Benbouzid, S. Liu, and F. Gao, "Two-stage distributionally robust optimization-based coordinated scheduling of integrated energy system with electricity-hydrogen hybrid energy storage," *Protection and Control of Modern Power Systems*, vol. 8, no. 2, pp. 1–14, 2023.

[44] S. A. Vomva, G. C. Kryonidis, A. I. Nousdilis, G. C. Christoforidis, and G. K. Papagiannis, "Integrated operation of droop controlled electrical networks with district heating networks," in *2022 2nd International Conference on Energy Transition in the Mediterranean Area (SyNERGY MED)*, 2022, pp. 1–6.

[45] Y. Chen and W. Wei, "Robust generation dispatch with strategic renewable power curtailment and decision-dependent uncertainty," *IEEE Transactions on Power Systems*, vol. 38, no. 5, pp. 4640–4654, 2023.

[46] B. Hong and Z. Zheng, "Stochastic multi-objective dynamic optimal dispatch for combined heat and power microgrid," in *2016 IEEE PES Asia-Pacific Power and Energy Engineering Conference (APPEEC)*, 2016, pp. 2369–2373.

[47] Y. Liu and N.-K. C. Nair, "A two-stage stochastic dynamic economic dispatch model considering wind uncertainty," *IEEE Transactions on Sustainable Energy*, vol. 7, no. 2, pp. 819–829, 2016.

[48] W. Kong, K. Sun, and J. Zhao, "Two-stage optimal scheduling of community integrated energy system considering operation sequences of hydrogen energy storage systems," *Journal of Modern Power Systems and Clean Energy*, vol. 13, no. 1, pp. 276–288, 2025.

[49] V. C. Pandey, N. Gupta, K. R. Niazi, and A. Swarnkar, "A scenario-based stochastic dynamic economic load dispatch considering wind uncertainty," in *2019 8th International Conference on Power Systems (ICPS)*, 2019, pp. 1–5.

[50] Y. Yang, W. Wu, B. Wang, and M. Li, "Chance-constrained economic dispatch considering curtailment strategy of renewable energy," *IEEE Transactions on Power Systems*, vol. 36, no. 6, pp. 5792–5802, 2021.

[51] S. Xu, W. Wu, Y. Yang, C. Lin, and Y. Liu, "Chance-constrained joint dispatch of generation and wind curtailment-load shedding schemes with large-scale wind power integration," *IEEE Transactions on Sustainable Energy*, vol. 14, no. 4, pp. 2220–2233, 2023.

[52] Y. Cheng, J. Su, X. Chang, Z. Li, Y. Xue, and H. Sun, "Optimal operation of integrated electricity and heat energy systems considering cyber-physical interaction," *IEEE Transactions on Smart Grid*, vol. 17, no. 1, pp. 205–216, 2026.

[53] L. Zhang, Y. He, H. Wu, and N. D. Hatziargyriou, "An optimal scheduling framework for integrated energy systems using deep reinforcement learning and deep learning prediction models," *IEEE Transactions on Smart Grid*, vol. 16, no. 6, pp. 4620–4634, 2025.

[54] Energi data service. [Online]. Available: https://www.energidataservice.dk/tso-electricity/consumptionpergridarea

[55] I. Sarbu, M. Mirza, and E. Crasmareanu, "A review of modelling and optimisation techniques for district heating systems," *International Journal of Energy Research*, vol. 43, no. 13, pp. 6572–6598, 2019. [Online]. Available: https://onlinelibrary.wiley.com/doi/abs/10.1002/er.4600

[56] S. van der Zwan and I. Pothof, "Operational optimization of district heating systems with temperature limited sources," *Energy and Buildings*, vol. 226, p. 110347, 2020. [Online]. Available: https://www.sciencedirect.com/science/article/pii/S0378778820308239

[57] S. Van Der Meulen, "Load management in district heating systems," *Energy and Buildings*, vol. 12, no. 3, pp. 179–189, 1988. [Online]. Available: https://www.sciencedirect.com/science/article/pii/0378778888900631

[58] F. U. Nazir, B. C. Pal, and R. A. Jabr, "A two-stage chance constrained volt/var control scheme for active distribution networks with nodal power uncertainties," *IEEE Transactions on Power Systems*, vol. 34, no. 1, pp. 314–325, 2019.

[59] A. Samadi, R. Eriksson, L. Söder, B. G. Rawn, and J. C. Boemer, "Coordinated active power-dependent voltage regulation in distribution grids with pv systems," *IEEE Transactions on Power Delivery*, vol. 29, no. 3, pp. 1454–1464, 2014.

[60] N. Growe-Kuska, H. Heitsch, and W. Romisch, "Scenario reduction and scenario tree construction for power management problems," in *2003 IEEE Bologna Power Tech Conference Proceedings,*, vol. 3, 2003, pp. 7 pp. Vol.3–.

[61] N. M. M. Razali and A. H. Hashim, "Backward reduction application for minimizing wind power scenarios in stochastic programming," in *2010 4th International Power Engineering and Optimization Conference (PEOCO)*, 2010, pp. 430–434.

[62] Y. Wang, Y. Liu, and D. S. Kirschen, "Scenario reduction with submodular optimization," *IEEE Transactions on Power Systems*, vol. 32, no. 3, pp. 2479–2480, 2017.

[63] M. L. Fisher, G. L. Nemhauser, and L. A. Wolsey, *An analysis of approximations for maximizing submodular set functions—II.* Berlin, Heidelberg: Springer Berlin Heidelberg, 1978, pp. 73–87. [Online]. Available: https://doi.org/10.1007/BFb0121195

[64] B. Schölkopf and A. J. Smola, *Learning with Kernels: Support Vector Machines, Regularization, Optimization, and Beyond.* The MIT Press, 12 2001. [Online]. Available: https://doi.org/10.7551/mitpress/4175.001.0001

[65] C. Bishop, *Pattern Recognition and Machine Learning*, 01 2006, vol. 16, pp. 140–155.

[66] I. Džafić, R. A. Jabr, E. Halilovic, and B. C. Pal, "A sensitivity approach to model local voltage controllers in distribution networks," *IEEE Transactions on Power Systems*, vol. 29, no. 3, pp. 1419–1428, 2014.

[67] A. Gopi and P. A.-D.-V. Raj, "Distributed generation for line loss reduction in radial distribution system," in *2012 International Conference on Emerging Trends in Electrical Engineering and Energy Management (ICETEEEM)*, 2012, pp. 29–32.

[68] Y. P. Agalgaonkar, B. C. Pal, and R. A. Jabr, "Distribution voltage control considering the impact of pv generation on tap changers and autonomous regulators," *IEEE Transactions on Power Systems*, vol. 29, no. 1, pp. 182–192, 2014.

Appendices

Appendix A

5-bus DHS system data

Both the heating networks, DHS1 and DHS2, utilised in the Chapter 4 have the same configurations and parameters. The heat network parameters, generation, and load details are listed in this appendix.

A.1 Heat network pipe parameters

Different parameters of the pipes are as follows:

Diameter = 0.15 m,

ϵ = 1.25 x 10 $^{-}$3 m,

λ = 0.2 W/mK,

μ = 0.294 x 10 $^{-}$6 m^2/s,

L = 100 m

Water density, ρ = 958.4 kg/m^3,

Specific heat of water, $c_p = 4182$ J/(kg.K),

A.2 Source and load details

Conventional heat source rating = 3 MW

Heat load power at bus 1 to 4 = 0.8 MW

Boiler efficiency = 95%

Lower bound on temperature at nodes 1 to 4 = 90 ^oC or 363 K

Upper bound on temperature at nodes 1 to 4 = 110 ^oC or 383 K

Appendix B

IEEE 15-bus system data

Table B.1: 15-bus system line data: resistance and reactance (pu) [67]

From bus	**To bus**	**Resistance (pu)**	**Reactance (pu)**
1	2	0.00315	0.075207
2	3	0.00033	0.001849
3	4	0.00667	0.038008
4	5	0.00579	0.014949
5	6	0.01414	0.036549
6	7	0.00800	0.039661
7	8	0.00900	0.041575
8	9	0.00700	0.032346

Continued on next page

Table B.1 – continued from previous page

From bus	To bus	Resistance (pu)	Reactance (pu)
9	10	0.03667	0.016964
10	11	0.00900	0.0415754
11	12	0.02750	0.127043
13	14	0.03150	0.081405
13	15	0.03965	0.102984
14	15	0.01061	0.004153

Table B.2: 15-bus system line data: active and reactive power flow (pu) [67]

From bus	To bus	P (pu)	Q (pu)
1	2	0.0208	0.0021
2	3	0.0495	0.0051
3	4	0.0958	0.0098
4	5	0.4222	0.0045
5	6	0.1383	0.0012

Continued on next page

Table B.2 – continued from previous page

From bus	To bus	P (pu)	Q (pu)
6	7	0.6538	0.0066
7	8	0.0323	0.0033
8	9	0.0213	0.0022
9	10	0.0280	0.0029
10	11	0.2170	0.0022
11	12	0.1330	0.0018
13	14	0.0029	0.0003
13	15	0.0161	0.0016
14	15	0.0139	0.0014

Appendix C

95-bus UKGDS data

Table C.1: 95-bus UKGDS line data [68]

From bus	To bus	Resistance (Ohm)	Reactance (Ohm)
1	2	0.0590359	0.0612018
2	3	0.1180355	0.4027364
3	4	0.2541000	0.2546300
4	5	0.3129060	0.2318433
5	6	0.1564530	0.1069156
6	7	0.3569500	0.1815000
7	8	0.4283400	0.2178000
8	9	0.3353636	0.1469182
Continued on next page			

Table C.1 – continued from previous page

From bus	To bus	Resistance (Ohm)	Reactance (Ohm)
9	10	0.1349029	0.0892496
10	11	0.4188052	0.2499013
11	12	0.4171959	0.2851244
13	14	0.2086040	0.1425622
14	15	0.3650499	0.2494778
15	16	0.4418557	0.1844524
16	17	0.1767447	0.0737858
17	18	0.3093002	0.1291191
18	19	0.2209218	0.0922262
19	20	0.3534773	0.1475595
20	21	0.3093002	0.1291191
21	22	0.5302220	0.2213453
22	23	0.2651110	0.1106666
23	24	0.0910041	0.0347996
24	25	0.1767447	0.0737858

Continued on next page

Table C.1 – continued from previous page

From bus	To bus	Resistance (Ohm)	Reactance (Ohm)
25	26	0.3534773	0.1475595
1	27	0.0664169	0.0688490
27	28	0.0469601	0.1258400
3	29	0.2095962	0.0918269
4	30	0.2934371	0.1285504
5	31	0.4192045	0.1836538
6	32	0.3650449	0.2494778
32	33	0.2346795	0.1603855
33	34	0.2868305	0.190200
34	35	0.3129060	0.2138433
35	36	0.1564530	0.1069156
36	37	0.2607550	0.1781967
37	38	0.2346795	0.1603855
38	39	0.3650449	0.2494778
39	40	0.1089000	0.1052700

Continued on next page

Table C.1 – continued from previous page

From bus	To bus	Resistance (Ohm)	Reactance (Ohm)
40	41	0.4356000	0.4210800
41	42	0.1452000	0.1403600
7	43	0.2515227	0.1101947
8	44	0.2934371	0.1285504
9	45	0.3129060	0.2138433
45	46	0.3772780	0.1652860
11	47	0.1888568	0.1249446
47	48	0.2698058	0.1784992
48	49	0.2583350	0.1104246
13	50	0.1427800	0.0726000
50	51	0.2855600	0.1452000
51	52	0.2141700	0.1089000
52	53	0.1137521	0.0434995
53	54	0.2141700	0.1089000
54	55	0.4283400	0.2178000

Continued on next page

Table C.1 – continued from previous page

From bus	To bus	Resistance (Ohm)	Reactance (Ohm)
55	56	0.4283400	0.2178000
56	57	0.3353636	0.1469182
57	58	0.6458254	0.2760736
14	59	0.2515227	0.1101947
59	60	0.5030454	0.2203773
60	61	0.3353636	0.1469182
15	62	0.3129060	0.2138433
62	63	0.1564530	0.1069156
63	64	0.2607550	0.1781967
64	65	0.2346795	0.1603855
65	66	0.3129060	0.2138433
66	67	0.0782265	0.0534578
67	68	0.3296524	0.0485452
68	69	0.1977866	0.0291247
69	70	0.1043020	0.0712811

Continued on next page

Table C.1 – continued from previous page

From bus	To bus	Resistance (Ohm)	Reactance (Ohm)
70	71	0.1825285	0.1247389
71	72	0.3296524	0.0485452
72	73	0.593371	0.0873862
16	74	0.2095962	0.0918269
74	75	0.3772780	0.1652860
18	76	0.2515227	0.1101947
21	77	0.1137521	0.0434995
25	78	0.4860328	0.2028928
33	79	0.2095962	0.0918269
34	80	0.2515227	0.1101947
35	81	0.1676818	0.0734591
36	82	0.2086040	0.1425622
82	83	0.1303775	0.0891044
40	84	0.1592481	0.0608993
50	85	0.2515227	0.1101947

Continued on next page

Table C.1 – continued from previous page

From bus	To bus	Resistance (Ohm)	Reactance (Ohm)
54	86	0.2855600	0.1452000
57	87	0.2583350	0.1104246
59	88	0.3353636	0.1469182
63	89	0.2209218	0.0922262
89	90	0.3534773	0.1475595
90	91	0.5302220	0.2138433
64	92	0.1564530	0.1069156
65	93	0.3353636	0.1469182
93	94	0.5868742	0.2571129
94	95	0.2737141	0.0567006

Table C.2: 95-bus UKGDS load data [67]

Bus number	Active power (kW)	Reactive power (kVAr)
1	940	170
		Continued on next page

Table C.2 – continued from previous page

Bus number	**Active power (kW)**	**Reactive power (kVAr)**
2	0	0
3	10	2
4	0	0
5	0	0
6	0	0
7	0	0
8	0	0
9	0	0
10	20	6
11	0	0
12	10	1
13	0	0
14	0	0
15	20	6
16	0	0

Continued on next page

Table C.2 – continued from previous page

Bus number	Active power (kW)	Reactive power (kVAr)
17	20	4
18	0	0
19	30	3
20	20	6
21	0	0
22	10	3
23	0	0
24	0	0
25	0	0
26	10	3
27	0	0
28	650	130
29	10	2
30	20	4
31	20	4

Continued on next page

Table C.2 – continued from previous page

Bus number	Active power (kW)	Reactive power (kVAr)
32	0	0
33	0	0
34	0	0
35	0	0
36	0	0
37	40	10
38	20	6
39	20	6
40	0	0
41	930	310
42	0	50
43	20	6
44	10	1
45	40	10
46	20	6

Continued on next page

Table C.2 – continued from previous page

Bus number	Active power (kW)	Reactive power (kVAr)
47	20	10
48	140	30
49	10	1
50	0	0
51	40	10
52	0	0
53	0	0
54	0	0
55	0	0
56	10	2
57	0	0
58	40	10
59	0	0
60	10	3
61	10	1

Continued on next page

Table C.2 – continued from previous page

Bus number	Active power (kW)	Reactive power (kVAr)
62	0	0
63	0	0
64	0	0
65	0	0
66	40	10
67	0	0
68	120	20
69	0	0
70	40	10
71	0	0
72	40	10
73	0	0
74	10	3
75	10	3
76	20	4

Continued on next page

Table C.2 – continued from previous page

Bus number	Active power (kW)	Reactive power (kVAr)
77	20	6
78	50	10
79	0	0
80	20	10
81	10	3
82	0	0
83	50	10
84	10	1
85	20	4
86	10	3
87	20	6
88	0	0
89	0	0
90	0	0
91	30	6

Continued on next page

Table C.2 – continued from previous page

Bus number	Active power (kW)	Reactive power (kVAr)
92	0	0
93	80	20
94	0	0
95	70	10